Journal of Computational Physics 228 (2009) 312–335

Contents lists available at ScienceDirect

Journal of Computational Physics

journal homepage: www.elsevier.com/locate/jcp

Absorbing boundary conditions for the one-dimensional Schrödinger equation with an exterior repulsive potential

Xavier Antoine [a,*], Christophe Besse [b], Pauline Klein [a]

[a] Institut Elie Cartan Nancy, Nancy-Université, CNRS UMR 7502, INRIA CORIDA Team, Boulevard des Aiguillettes B.P. 239, F-54506 Vandoeuvre-lès-Nancy, France
[b] Equipe Projet Simpaf – Inria CR Lille Nord Europe, Laboratoire Paul Painlevé, Unité Mixte de Recherche CNRS (UMR 8524), UFR de Mathématiques Pures et Appliquées, Université des Sciences et Technologies de Lille, Cité Scientifique, 59655 Villeneuve d'Ascq Cedex, France

ARTICLE INFO

Article history:
Received 11 June 2008
Received in revised form 10 September 2008
Accepted 11 September 2008
Available online 25 September 2008

Keywords:
Schrödinger equation
Artificial boundary condition
Exterior potential
Unconditionally stable discretization schemes
Numerical simulations

ABSTRACT

Mathematical constructions and comparisons of accurate absorbing boundary conditions for the one-dimensional Schrödinger equation with a general variable repulsive potential are developed. Stable semi-discretization schemes are built for the associated initial boundary value problems. Finally, some numerical simulations give a comparison of the various absorbing boundary conditions and show that they yield accurate computations.

1. Introduction

We consider in this paper the following initial value problem which consists in a time-dependent Schrödinger equation with potential V set in an unbounded domain

$$\begin{aligned} &i\partial_t u + \partial_x^2 u + Vu = 0, \quad (x,t) \in \mathbb{R} \times [0;T], \\ &u(x,0) = u_0(x), \qquad\quad x \in \mathbb{R}, \end{aligned} \tag{1}$$

where u_0 is the initial data. The maximal time of computation is denoted by T. We assume here that V is a real-valued potential such that $V \in \mathcal{C}^\infty(\mathbb{R} \times \mathbb{R}^+, \mathbb{R})$. Finally, we make the assumption that V is a repulsive potential [10]. This kind of potential then creates acceleration of the field compared to the free-potential equation [10,8,20,21].

For obvious reasons linked to the numerical solution of such problems, it is usual to truncate the spatial domain with a fictitious boundary $\Sigma := \partial\Omega = \{x_l, x_r\}$, where x_l and x_r, respectively, designate the left and right endpoints introduced to have a bounded domain of computation $\Omega =]x_l; x_r[$. Let us introduce the time domains $\Omega_T = \Omega \times [0;T]$ and $\Sigma_T = \Sigma \times [0;T]$. Considering the fictitious boundary Σ, we are now led to solve the problem

$$\begin{aligned} &i\partial_t u + \partial_x^2 u + Vu = 0, \quad (x,t) \in \Omega_T, \\ &u(x,0) = u_0(x), \qquad\quad x \in \Omega. \end{aligned} \tag{2}$$

* Corresponding author. Tel.: +33 3 83 68 45 34; fax: +33 5 61 55 83 85.
E-mail addresses: Xavier.Antoine@iecn.u-nancy.fr (X. Antoine), Christophe.Besse@math.univ-lille1.fr (C. Besse), Pauline.Klein@iecn.u-nancy.fr (P. Klein).

0021-9991/$ - see front matter © 2008 Elsevier Inc. All rights reserved.
doi:10.1016/j.jcp.2008.09.013

In the sequel of the paper, we assume that the initial datum u_0 is compactly supported in the computational domain Ω.

Of course, a boundary condition set on Σ_T must be added to system (2). An ideal boundary condition answering the problem is the so-called transparent boundary condition (TBC) which leads to a solution of (2) equal to the restriction of the solution of (1) on Ω_T. A first well-known case considers $V = 0$. This situation has been treated by many authors [2]. In this case, using a Laplace transform in time on (1), solving the associated Helmholtz-type differential equation in x and going back to the initial domain by inverse Laplace transform yields the following TBC in term of the Dirichlet-to-Neumann (DtN) operator

$$\partial_{\mathbf{n}} u + \mathrm{e}^{-\mathrm{i}\pi/4}\partial_t^{1/2} u = 0, \quad \text{on } \Sigma_T, \tag{3}$$

where $\mathbf{n}$ is the outwardly directed unit normal vector to Σ. The operator $\partial_t^{1/2}$ is known as the half-order derivative operator (see Eq. (12) for its definition). Its nonlocal character related to its convolutional structure has led to many developments concerning its accurate and efficient evaluation in the background of TBCs [2].

A second situation which is related to the above case is when the potential is only time varying: $V(x,t) = V(t)$. In this case, the change of unknown

$$v(x,t) = \mathrm{e}^{-\mathrm{i}\mathcal{V}(t)} u(x,t), \tag{4}$$

with

$$\mathcal{V}(t) = \int_0^t V(s)\mathrm{d}s \tag{5}$$

reduces the initial Schrödinger equation with potential to the free-potential Schrödinger equation [5]. Then, the TBC (3) can be used for v and the resulting DtN TBC for u is

$$\partial_{\mathbf{n}} u(x,t) + \mathrm{e}^{-\mathrm{i}\pi/4}\mathrm{e}^{\mathrm{i}\mathcal{V}(t)}\partial_t^{1/2}\left(\mathrm{e}^{-\mathrm{i}\mathcal{V}(t)} u(x,t)\right) = 0, \quad \text{on } \Sigma_T. \tag{6}$$

In the two above situations, the potential does not depend on the spatial variable x. Very recently, some attempts have been directed towards the derivation of TBCs for special potentials. In [18], the case of a linear potential is considered in the background of parabolic equations in electromagnetism. Using the Airy functions, the TBC can still be written explicitly and its accuracy is tested. Again, for the linear potential, improvements have been introduced in [12] using a discrete transparent boundary condition. In [27], Zheng derives the TBC in the special case of a sinusoidal potential using Floquet's theory. Extensions to two-dimensional PDEs problems have been proposed in [13]. Finally, in [14], the authors consider the case of a Coulomb-like potential which can be handled explicitly in the TBC by means of the Whitaker's second functions. All these solutions take care of the very special form of the potential. Let us remark that other solutions based on PML techniques have also been recently proposed e.g. in [26].

To the best of our knowledge, the problem of considering a solution in the case of a general potential has not been yet addressed. We must notice here that a general theory cannot be expected to provide a general TBC. A more realistic goal is to build an accurate approximation of the TBC which is usually called artificial or Absorbing Boundary Condition (ABC). The aim of this paper is to prospect different ways of building such boundary conditions and to approximate them correctly to get unconditionally stable numerical schemes.

The paper is organized as follow. In Section 2, we present two possible approaches for building ABCs for the one-dimensional Schrödinger equation with a variable repulsive potential. The central key point of these approaches is based on a derivation of a suitable asymptotic expansion of the related Dirichlet-to-Neumann (DtN) operator. Therefore, after giving the basic tools of fractional pseudodifferential operators, we derive in Section 2.2 some asymptotic of the DtN map for our equation taking care of the principal symbol. Numerical formal comparisons are provided in the case of a linear potential. Next, Section 2.3 discusses the choice of the ABC and some modifications of the asymptotic expansions yielding a first class of second- and fourth-orders ABCs. A well-posedness result is then stated in Section 2.4. A second family of ABCs is proposed in Section 2.5. It is shown in Section 2.6 that these ABCs can be identified to the first ones if and only if the potential is time independent. Otherwise, these new conditions yield different formulations. We consider in Section 3 the semi-discretization of the various ABCs and state unconditional stability results for the first class of ABCs. Additional (symbolic) approximations of the second family of ABCs are introduced in view of an efficient discretization. Section 4 presents some numerical computations for time dependent and time independent space variable potentials. These simulations show the high accuracy and effectiveness of the proposed ABCs. Moreover, comparisons are provided between the two approaches. Finally, a conclusion is given in Section 5.

2. Artificial boundary conditions for a general potential

2.1. Two possible approaches

The first natural strategy would consists in building an approximate boundary condition based on Eq. (1) with unknown u.

A second strategy is the following. Let us consider now that u is the exact solution of (1) and let us define the phase function $\mathcal{V}$ as a primitive in time of the potential V

$$\mathcal{V}(x,t) = \int_0^t V(x,s)\mathrm{d}s. \tag{7}$$

Let us introduce v as the new unknown defined by

$$v(x,t) = \mathrm{e}^{-\mathrm{i}\mathcal{V}(x,t)}u(x,t). \tag{8}$$

We obviously have $v_0(x) = u_0(x)$. Moreover, plugging u given by (7) and (8) into the Schrödinger equation with potential shows that v is solution to the variable coefficient Schrödinger equation

$$\mathrm{i}\partial_t v + \partial_x^2 v + f\partial_x v + gv = 0, \quad \text{in } \Omega_T, \tag{9}$$

setting $f = 2\mathrm{i}\partial_x\mathcal{V}$ and $g = \mathrm{i}\partial_x^2\mathcal{V} - (\partial_x\mathcal{V})^2$. The fundamental reason why considering this change of unknown is crucial is that this first step would lead to the TBC applied to v and associated to (9) for a time-dependent but *x-independent* potential (since then $f = g = 0$). This is not the case if we work directly with the initial unknown u for (2) which would give an approximate artificial boundary condition even for a time-dependent and *x-independent* potential. Let us note that this strategy (called "Phase Function Transformation Strategy" in [2]) has been first applied with success in [5] for nonlinear artificial boundary conditions for the one-dimensional nonlinear Schrödinger equation.

We will see later that these approaches lead to different artificial boundary conditions which however coincide in some cases.

2.2. Derivation of the asymptotic expansion of the DtN operator

2.2.1. Fractional pseudodifferential operators

Since the Schrödinger equation has a space-time potential, it is well-known that an approach purely based on the Laplace transform is inadequate. Furthermore, for a x-dependent potential $V(x,t) = V(x)$, being able to build the TBC would require the solution of a second-order Helmholtz-type differential equation after applying a Laplace transform. This is impossible in general for a given potential. This is the reason why trying to build an approximate boundary condition is more realistic. To this end, we propose an approach based on the theory of pseudodifferential operators which naturally generalizes the Laplace transform and the use of a factorization theorem which gives an approximate solution to the second-order differential equation in x. This approach is strongly related to the pioneering works of Engquist and Majda [15] for other kinds of PDEs.

A pseudodifferential operator $P(x,t,\partial_t)$ is given by its symbol $p(x,t,\tau)$ in the Fourier space

$$P(x,t,\partial_t)u(x,t) = \mathcal{F}_t^{-1}(p(x,t,\tau)\hat{u}(x,\tau)) = \int_{\mathbb{R}} p(x,t,\tau)\mathcal{F}_t(u)(x,\tau)\mathrm{e}^{\mathrm{i}t\tau}\,\mathrm{d}\tau, \tag{10}$$

where $\mathcal{F}_t$ is the time Fourier transform

$$\mathcal{F}_t(u)(x,\tau) = \frac{1}{2\pi}\int_{\mathbb{R}} u(x,t)\mathrm{e}^{-\mathrm{i}t\tau}\,\mathrm{d}t.$$

The inhomogeneous pseudodifferential operator calculus that we use in the paper was introduced in [17] and applied e.g. in [3]. For the sake of conciseness, we only give the useful material needed here. Let α be a real number and Ξ an open subset of $\mathbb{R}$. Then (see in [24]), the symbol class $S^\alpha(\Xi\times\Xi)$ denotes the linear space of $\mathcal{C}^\infty$ functions $a(x,t,\tau)$ in $\Xi\times\Xi\times\mathbb{R}$ such that for each $K\subseteq\Xi\times\Xi$ and that for all indices β, δ, γ, there exists a constant $C_{\beta,\delta,\gamma}(K)$ such that

$$|\partial_\tau^\beta\partial_t^\delta\partial_x^\gamma a(x,t,\tau)| \leqslant C_{\beta,\delta,\gamma}(K)(1+|\tau|^2)^{\alpha-\beta},$$

for all $(x,t)\in K$ and $\tau\in\mathbb{R}$. A function f is said to be inhomogeneous of degree m if: $f(x,t,\mu\tau) = \mu^m f(x,t,\tau)$, for any $\mu > 0$. Then, a pseudodifferential operator $P = P(x,t,\partial_t)$ is inhomogeneous and classical of order M, $M\in\mathbb{Z}/2$, if its total symbol, designated by $p = \sigma(P)$, has an asymptotic expansion in inhomogeneous symbols $\{p_{M-j/2}\}_{j=0}^{+\infty}$ as

$$p(x,t,\tau) \sim \sum_{j=0}^{+\infty} p_{M-j/2}(x,t,\tau),$$

where each function $p_{M-j/2}$ is inhomogeneous of degree $M-j/2$, for $j\in\mathbb{N}$. The meaning of $\sim$ is that

$$\forall\tilde{m}\in\mathbb{N}, \quad p - \sum_{j=0}^{\tilde{m}} p_{M-j/2} \in S^{M-(\tilde{m}+1)/2}.$$

A symbol p satisfying the above property is quoted by $p\in S_S^M$ and the associated operator $P = Op(p)$ by inverse Fourier transform by $P\in \mathrm{OPS}_S^M$. Finally, let us remark that smoothness of the potential V is required for applying pseudodifferential operators theory. However, this is crucial into the complementary set of Ω but a much weaker regularity hypothesis could be expected for the interior problem set in Ω allowing therefore a wide class of potentials.

Other useful nonlocal operators in the sequel of the paper are the fractional integration operators $I_t^{\alpha/2}$ of order $\alpha/2$ which are defined by the relation

$$I_t^{\alpha/2} f(t) = \frac{1}{\Gamma(\alpha/2)} \int_0^t (t-s)^{\alpha/2-1} f(s) \mathrm{d}s, \quad \text{for } \alpha \in \mathbb{N} \tag{11}$$

and have Fourier symbol $(\frac{i}{\tau})^{\alpha/2}$, where Γ designates the Gamma special function. Another operator is the fractional differential operator $\partial_t^{1/2}$ given by

$$\partial_t^{1/2} f(t) = \frac{1}{\sqrt{\pi}} \partial_t \int_0^t \frac{f(s)}{\sqrt{t-s}} \mathrm{d}s, \tag{12}$$

with symbol $\mathrm{e}^{\mathrm{i}\pi/4}\sqrt{\tau}$. All along the paper, we consider that, for a complex number z, $\sqrt{z}$ is the principal determination of the square-root with branch-cut along the negative real axis.

One of the key points of pseudodifferential operator calculus is that it enables to manipulate symbols of operators at the algebraic level rather than operators at the functional level, therefore giving practical rules of computation e.g. for the composition of two variable coefficients integro-differential operators (that is with non polynomial symbols in τ).

2.2.2. Computation of the asymptotic symbolic expansion of the DtN operator

For conciseness, we explain here how to compute the asymptotic expansion of the DtN operator for a given model Schrödinger equation with smooth variable coefficients A and B

$$L(x,t,\partial_x,\partial_t)w = \mathrm{i}\partial_t w + \partial_x^2 w + A\partial_x w + Bw = 0. \tag{13}$$

Since we are trying to build an approximation of the DtN operator at the boundary, we must be able to write the normal derivative trace operator ∂_x (focusing on the right point x_r) as a function of the trace operator through an operator Λ^+ which involves some (fractional) time derivatives of w as well as the effect of the potential V and its (x,t) variations. This can be done in an approximate way thanks to the factorization of L given by relation (13)

$$L(x,t,\partial_x,\partial_t) = (\partial_x + \mathrm{i}\Lambda^-)(\partial_x + \mathrm{i}\Lambda^+) + R, \tag{14}$$

where $R \in \mathrm{OPS}^{-\infty}$ is a smoothing pseudodifferential operator. The operators $\Lambda^\pm$ are pseudodifferential operators of order 1/2 (in time) and order zero in x. Computing the operators $\Lambda^\pm$ in an exact way through their respective total symbols $\sigma(\Lambda^\pm)$ cannot be expected in general. Therefore, an asymptotic form of the total symbol $\sigma(\Lambda^\pm)$ is sought as

$$\sigma(\Lambda^\pm) = \lambda^\pm \sim \sum_{j=0}^{+\infty} \lambda^\pm_{1/2-j/2}, \tag{15}$$

where $\lambda^\pm_{1/2-j/2}$ are symbols corresponding to operators of order $1/2 - j/2$.

Now, expanding the factorization (14), identifying the terms in L in front of the ∂_x operators with the ones from the expanded factorization and finally using a few symbolic manipulations yield the system of equations

$$\begin{cases} \mathrm{i}(\lambda^- + \lambda^+) = a, \\ \mathrm{i}\partial_x \lambda^+ - \sum\limits_{\alpha=0}^{\infty} \frac{(-\mathrm{i})^\alpha}{\alpha!} \partial_\tau^\alpha \lambda^- \partial_t^\alpha \lambda^+ = -\tau + b, \end{cases} \tag{16}$$

with $a(x,t) = \sigma(A) = A$, $b(x,t) = \sigma(B) = B$, since A and B are two functions of (x,t).

Looking at the first equation of system (16), we see that we must have: $\lambda^-_{1/2} = -\lambda^+_{1/2}$. Now, if we identify the highest order symbol in the second equation of system (16), then one gets four possibilities

$$\lambda^+_{1/2}(\tau) = \mp\sqrt{-\tau} \tag{17}$$

or

$$\lambda^+_{1/2}(x,t,\tau) = \mp\sqrt{-\tau + b(x,t)}. \tag{18}$$

The first choice can be viewed as considering a principal classical symbol and the second possibility yields a semi-classical symbol (following the notations e.g. in [10]). Let us now adopt the first strategy which consists in working on Eq. (1) for u setting $A = 0$ and $B = V$. Following e.g. [2], the principal symbol with negative imaginary part characterizes the outgoing part of the wave field u. Studying the sign of (17) and (18) for a real-valued potential V shows that the negative sign gives the good choice. Therefore, we obtain the two possible symbols

$$\lambda^+_{1/2} = -\sqrt{-\tau} \tag{19}$$

and

$$\lambda^+_{1/2} = -\sqrt{-\tau + V}. \tag{20}$$

Let us now consider the second choice based on the gauge change leading to compute v solution to (9) for $A = f$ and $B = g$. Then, again, choosing (19) yields the outgoing solution for v. However, g is now a complex-valued potential with no fixed sign. Therefore, we cannot determine the outgoing wave for (18).

Choosing the principal symbol is a crucial point since it is directly related to the accuracy of the artificial boundary condition. Moreover, for a given choice of the principal symbol, the corrective asymptotic terms $\{\lambda^+_{1/2-j/2}\}_{j\geqslant 1}$ are different since they are computed in cascade developing the infinite sum in the second equation of (16). For the first strategy, we have the following proposition.

Proposition 1. *Let us fix $\lambda^+_{1/2}$ by the expression (19). Then, the solution to system (16) is given by*

$$\lambda^+_0 = \frac{1}{2\lambda^+_{1/2}}\left(-\mathrm{i}\partial_x\lambda^+_{1/2} - \mathrm{i}a\lambda^+_{1/2}\right) \tag{21}$$

and, for $j \in \mathbb{N}$, $j \geqslant 1$, by

$$\lambda^+_{-j/2} = \frac{1}{2\lambda^+_{1/2}}\left(b\delta_{j,1} - \mathrm{i}\partial_x\lambda^+_{-j/2+1/2} - \mathrm{i}a\lambda^+_{-j/2+1/2} - \sum_{k=1}^{j}\lambda^+_{-j/2+k/2}\lambda^+_{1/2-k/2} - \sum_{\alpha=1}^{(j+1)/2}\frac{(-\mathrm{i})^\alpha}{\alpha!}\sum_{k=0}^{j+1-2\alpha}\partial_\tau^\alpha\lambda^+_{-j/2+k/2+\alpha}\partial_t^\alpha\lambda^+_{1/2-k/2}\right), \tag{22}$$

where $\delta_{j,1} = 0$ if $j \neq 1$ and $\delta_{1,1} = 1$.

Applying the above proposition to our situation, one obtains the following corollary.

Corollary 1. *If we fix the principal symbol $\lambda^+_{1/2} = -\sqrt{-\tau}$ for $a = f$ and $b = g$, then the next three terms of the asymptotic symbolic expansion are given by*

$$\lambda^+_0 = \partial_x\mathcal{V}, \quad \lambda^+_{-1/2} = 0 \quad \text{and} \quad \lambda^+_{-1} = \frac{\mathrm{i}\partial_x V}{4\tau}. \tag{23}$$

For the second choice (18), the first symbols of the asymptotic expansion are given by the following proposition.

Proposition 2. *If one considers $\lambda^+_{1/2} = -\sqrt{-\tau + V}$ in (16) for $a = 0$ and $b = V$, then one has*

$$\lambda^+_0 = 0, \quad \lambda^+_{-1/2} = 0, \quad \text{and} \quad \lambda^+_{-1} = \frac{-\mathrm{i}}{4}\frac{\partial_x V}{-\tau + V}. \tag{24}$$

Remark 1. We cannot obtain a general expression similar to (22) for the second choice. The reason is that the terms appearing in (16) may be inhomogeneous. Indeed, derivating the symbols λ^+_j may lead to a sum of several terms of different orders. This is the case for example for $\partial_x\lambda^+_{-1}$, which is the sum of two terms, one of order -1 and the other of order -2.

Remark 2. Considering $\lambda^+_{1/2} = -\sqrt{-\tau}$ in (16) for $a = 0$ and $b = V$ would give some symbols which are approximations of $\lambda^+_{1/2} = -\sqrt{-\tau + V}$ and (24) by using a second-order truncated Taylor expansion when $|\tau| \to +\infty$. For this reason, this case which leads to less accurate artificial boundary conditions will not be considered in the sequel.

2.2.3. Comparison of the exact and approximate symbols for a linear potential

In the case of a linear potential $V = x$, the total symbol $\lambda^+(x,\tau)$ can be computed. It is thus possible to compare it to its asymptotic expansion based on (24). Applying a Fourier transform to Eq. (2) yields

$$\partial_x^2\hat{u} + (-\tau + x)\hat{u} = 0. \tag{25}$$

According to [18], the outgoing solution to (25) is

$$\hat{u}(x,\tau) = \mathrm{Ai}\left((x-\tau)\mathrm{e}^{-\mathrm{i}\pi/3}\right), \tag{26}$$

where Ai stands for the Airy function [1]. Derivating this expression, we obtain

$$\partial_{\mathbf{n}}\hat{u}(x,\tau) = \mathrm{e}^{-\mathrm{i}\pi/3}\frac{\mathrm{Ai}'\left((x-\tau)\mathrm{e}^{-\mathrm{i}\pi/3}\right)}{\mathrm{Ai}((x-\tau)\mathrm{e}^{-\mathrm{i}\pi/3})}\hat{u}(x,\tau), \tag{27}$$

which means that the total symbol of the DtN operator is

$$\lambda^+ = \mathrm{e}^{2\mathrm{i}\pi/3}\frac{\mathrm{Ai}'\left((x-\tau)\mathrm{e}^{-\mathrm{i}\pi/3}\right)}{\mathrm{Ai}((x-\tau)\mathrm{e}^{-\mathrm{i}\pi/3})}. \tag{28}$$

The application of Corollary 2 gives the first-order and second-order approximate symbols

$$\begin{aligned}\sigma_1 &= \mathrm{i}\lambda^+_{1/2} = -\mathrm{i}\sqrt{-\tau + x},\\ \sigma_2 &= \mathrm{i}\left(\lambda^+_{1/2} + \lambda^+_0 + \lambda^+_{-1/2} + \lambda^+_{-1}\right) = \sigma_1 + \tfrac{1}{4}\tfrac{1}{-\tau+x},\end{aligned} \tag{29}$$

setting $V = x$.

Let us fix the boundary condition at $x_r = 10$. For comparison, we draw on the two pictures of Fig. 1 the three symbols (28) and (29) in the complex plane for values of τ in $[-50; 0]$ (left) and $[0; 50]$ (right). For negative values of τ, we observe an

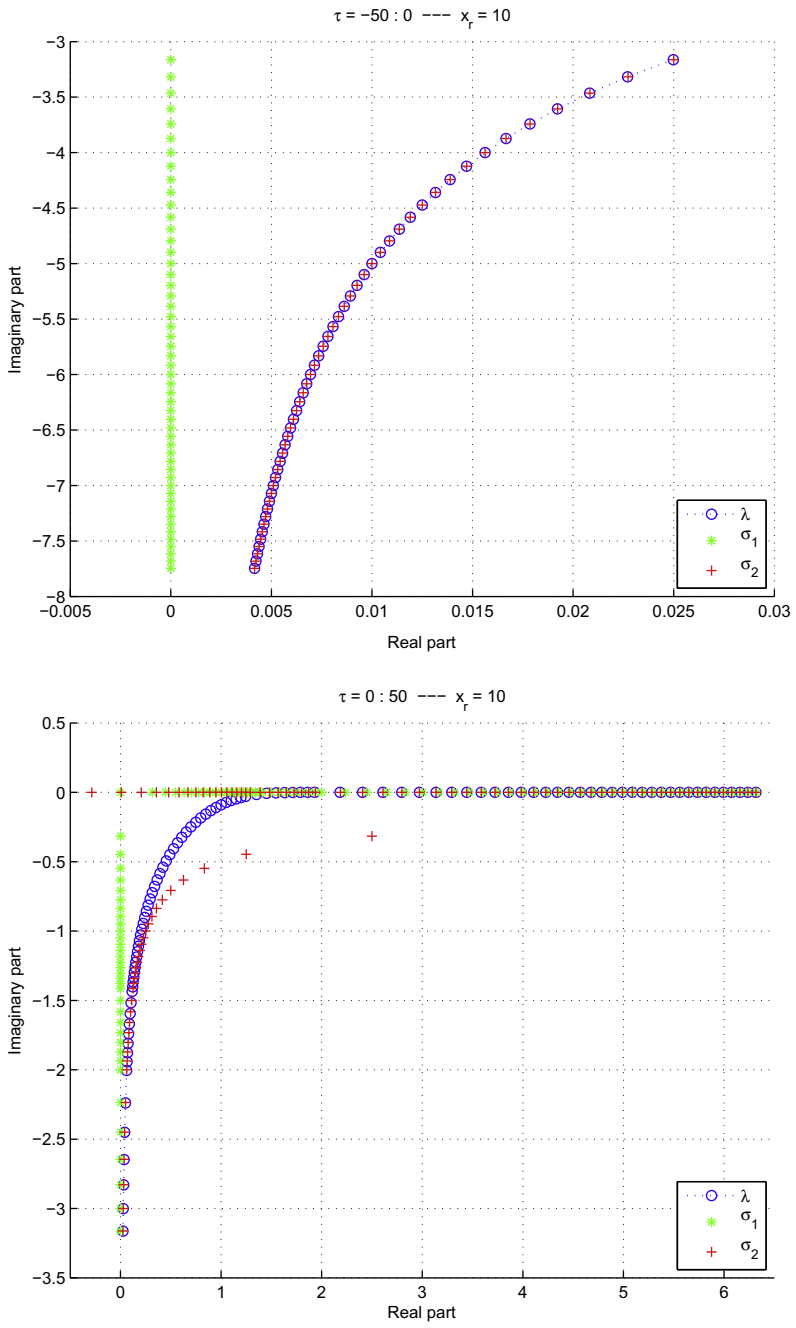

Fig. 1. Comparison of the exact total symbol λ^+ and its first- and second-order asymptotic approximations σ_1 and σ_2 in the complex plane at $x_r = 10$ and for $\tau \in [-50; 0]$ (left picture) and $\tau \in [0; 50]$ (right picture).

important correction when considering σ_2 instead of σ_1. The order of accuracy is about 10^{-5} for $|\tau| = 50$ (see Fig. 2). For positive values of τ we can see that the approximation of the symbol λ^+ is again improved when σ_2 is considered instead of σ_1. However, for both approximations, a singularity appears for $\tau = x_r$ while it is not the case for λ^+ which is smooth. This is the most dominant error in the approximation process of the symbols (see Fig. 2) and as a consequence in the construction of the artificial boundary condition. Finally, the error decays when $|\tau|$ is large (see Fig. 2) which is coherent with the asymptotic expansion (15) of the symbol λ^+. In particular, the symbols $\lambda^+_{1/2}$ and λ^+_{-1} given by the symbolic calculus rules are exactly the first terms of the asymptotic expansion of λ^+ in terms of Airy functions (28) for large values of τ (see e.g. [1] Chapter 10, properties 10.4.58, 10.4.59 and 10.4.61 p. 448).

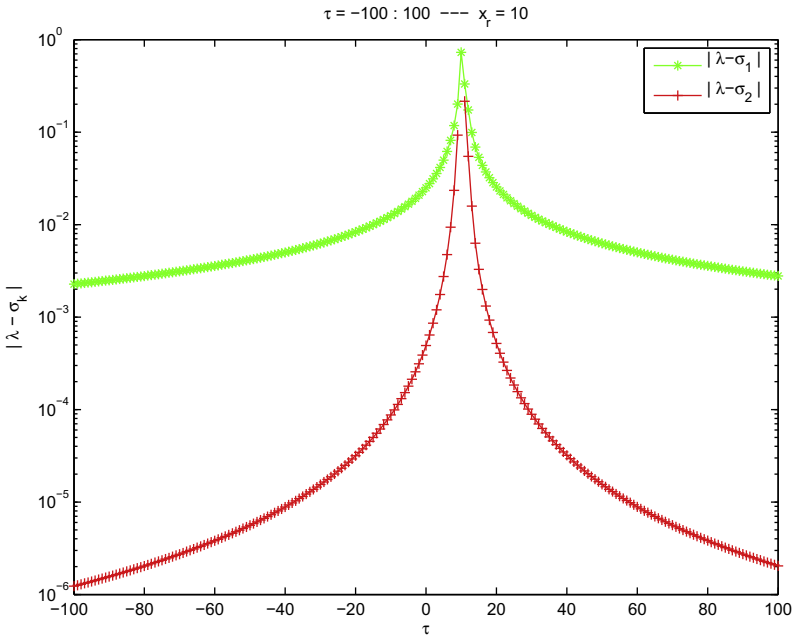

Fig. 2. Logarithm of the absolute error $|\lambda^+ - \sigma_1|$ and $|\lambda^+ - \sigma_2|$ with respect to τ. A singularity is observed at point $\tau = x_r = 10$.

2.3. Choosing the ABC

If we assume that V is a real-valued smooth function, then the $L^2(\mathbb{R})$-norm of the solution u to system (1) is conserved. If we truncate the domain by introducing a fictitious boundary, then one can expect that the $L^2(\Omega)$-norm of the solution is bounded by $\|u_0\|_{L^2(\Omega)}$. This is for example proved in [4] in the case of the free-potential. In the case of a general potential, the expression of the artificial boundary condition is essential in the proof of a similar result. In particular, by adapting the proof given in [7] using the Plancherel theorem for Laplace transform, the following Lemma is the keypoint for proving a well-posedness result.

Lemma 1. *Let $\varphi \in H^{1/4}(0,T)$ be a function extended by zero for any time $s > T$. Then, we have the following properties:*

$$\Re\left(e^{i\pi/4}\int_0^\infty \bar{\varphi}\ \partial_t^{1/2}\varphi\, dt\right) \geqslant 0,$$
$$\Re\left(\int_0^{+\infty} \bar{\varphi} I_t \varphi\, dt\right) = 0.$$

This Lemma emphasizes the fact that the artificial boundary condition must have a symmetrical form. Since our approach gives the principal symbol of an operator, an infinite choice of corresponding operators with this principal symbol is possible. For symmetrization reasons, we propose to fix the choice of the artificial boundary condition based on the principal symbol $\lambda^+_{1/2} = -\sqrt{-\tau}$ and (23) as follows:

Cancelling the outgoing wave corresponding to $\lambda^+_{1/2}$ for v writes down

$$\partial_{\mathbf{n}} v + i\Lambda^+ v = 0, \quad \text{on } \Sigma_T. \tag{30}$$

Retaining the M first symbols $\{\lambda^+_{1/2-j/2}\}_{M-1\geqslant j\geqslant 0}$, we consider the associated artificial boundary condition

$$\partial_{\mathbf{n}} u_M - i(\partial_x \mathcal{V}) u_M + ie^{i\mathcal{V}} \sum_{j=0}^{M-1} Op\left(\lambda^+_{1/2-j/2}\right)\left(e^{-i\mathcal{V}} u_M\right) = 0, \quad \text{on } \Sigma_T, \tag{31}$$

after replacing v in (30) by its expression (8). In Eq. (31), u_M designates an approximation of u since we do not have a Transparent Boundary Condition. However, u_M will be denoted by u in the sequel for conciseness. We adopt the following compact notation of (31)

$$\partial_{\mathbf{n}} u + \Lambda^M_\ell(x,t,\partial_t)u = 0, \quad \text{on } \Sigma_T, \tag{32}$$

where $M \geqslant 1$ corresponds to the order of the boundary condition and is equal to the total number of terms $\lambda^+_{j/2}$ retained in the sum. The subscript $\ell = 0$ (respectively $\ell = 1$) refers to the choice (19) (respectively (20)) of the principal symbol $\lambda^+_{1/2}$.

Let us begin by considering $\ell = 0$ and $M = 2$. Then one directly obtains

$$\Lambda_0^2(x,t,\partial_t)u = \mathrm{e}^{-\mathrm{i}\pi/4}\mathrm{e}^{\mathrm{i}\mathcal{V}(x,t)}\partial_t^{1/2}\left(\mathrm{e}^{-\mathrm{i}\mathcal{V}(x,t)}u\right), \tag{33}$$

which is a symmetrical operator. The case $M = 4$ is more ambiguous. Indeed, we only have access to the principal symbol $\lambda_{-1}^{+} = \frac{i\partial_x V}{4\tau}$ of an operator. A first possible choice would consist in considering that

$$Op(\lambda_{-1}^{+})v = \frac{\partial_{\mathbf{n}} V}{4} I_t v \mod(\mathrm{OPS}_S^{-3/2}). \tag{34}$$

(If A and B are two pseudodifferential operators of order α then we write $A = B \mathrm{mod}(\mathrm{OPS}^{\beta})$ to designate that $A - B$ are equal modulo a pseudodifferential operator of OPS^{β}, $\beta < \alpha$. A similar notation will be adopted at the symbol level: $\sigma_A = \sigma_B \mod(\mathrm{S}^{\beta})$.) However, the operator in the right-hand side is not symmetrical. Well-posedness results can be however stated with such a choice but under some very restrictive assumptions on V. A better choice of operator is

$$Op(\lambda_{-1}^{+})v = \mathrm{sg}(\partial_{\mathbf{n}} V)\frac{\sqrt{|\partial_{\mathbf{n}} V|}}{2} I_t\left(\frac{\sqrt{|\partial_{\mathbf{n}} V|}}{2} v\right) \mod(\mathrm{OPS}_S^{-3/2}), \tag{35}$$

which is symmetrical unlike (34) and leads to a well-posedness result under weaker assumptions. In the above equation, $\mathrm{sg}(\cdot)$ designates the sign function.

We finally obtain the following proposition:

Proposition 3. *For $\ell = 0$, the artificial boundary condition of order M is given by*

$$\partial_{\mathbf{n}} u + \Lambda_0^M u = 0, \quad \text{on } \Sigma_T, \tag{36}$$

with

$$\Lambda_0^2(x,t,\partial_t)u = \mathrm{e}^{-\mathrm{i}\pi/4}\mathrm{e}^{\mathrm{i}\mathcal{V}(x,t)}\partial_t^{1/2}\left(\mathrm{e}^{-\mathrm{i}\mathcal{V}(x,t)}u\right) \tag{37}$$

and

$$\Lambda_0^4(x,t,\partial_t)u = \Lambda_0^2(x,t,\partial_t)u + i\mathrm{sg}(\partial_{\mathbf{n}} V)\frac{\sqrt{|\partial_{\mathbf{n}} V|}}{2}\mathrm{e}^{\mathrm{i}\mathcal{V}(x,t)} I_t\left(\frac{\sqrt{|\partial_{\mathbf{n}} V|}}{2}\mathrm{e}^{-\mathrm{i}\mathcal{V}(x,t)}u\right). \tag{38}$$

The boundary condition (36) is referred to as ABC_0^M in the sequel.

2.4. A well-posedness result for ABC_0^M

Considering the artificial boundary conditions (36) of Proposition (3), we get the following well-posedness result.

Proposition 4. *Let $u_0 \in L^2(\Omega)$ be a compactly supported initial datum such that $\mathrm{Supp}(u_0) \subset \Omega$. Let $V \in \mathcal{C}^{\infty}(\mathbb{R}\times\mathbb{R}^+,\mathbb{R})$ be a real-valued potential. Let us denote by u a solution of the initial boundary value problem*

$$\begin{cases} \mathrm{i}\partial_t u + \partial_x^2 u + Vu = 0, & \text{in } \Omega_T, \\ \partial_{\mathbf{n}} u + \Lambda_0^M u = 0, & \text{on } \Sigma_T, \\ u(x,0) = u_0(x), & \forall x \in \Omega, \end{cases} \tag{39}$$

where the operators Λ_0^M, $M = 2, 4$, are defined in Proposition 3. Then, u fulfils the following energy bound:

$$\forall t > 0, \quad \|u(t)\|_{L^2(\Omega)} \leqslant \|u_0\|_{L^2(\Omega)}, \tag{40}$$

for $M = 2$. Moreover, if $\mathrm{sg}(\partial_{\mathbf{n}} V)$ is constant on Σ_T, then the inequality (40) holds for $M = 4$. In particular, this implies that we have the uniqueness of the solution u of the initial boundary value problem (39).

Proof. Let us multiply the Schrödinger equation by $-\mathrm{i}\bar{u}$, and integrate by parts on Ω. We obtain the following equation:

$$\partial_t \int_{x_l}^{x_r} \frac{|u|^2}{2}\mathrm{d}x - \mathrm{i}[\bar{u}\partial_{\mathbf{n}} u]_{x_l}^{x_r} + \mathrm{i}\int_{x_l}^{x_r} |\partial_x u|^2 \mathrm{d}x - \mathrm{i}\int_{x_l}^{x_r} V(x,t)|u|^2 \mathrm{d}x = 0. \tag{41}$$

Taking the real part of the above expression and integrating on an arbitrary time interval $[0;T]$ leads to

$$\frac{1}{2}\left(\|u(T)\|_{L^2(\Omega)}^2 - \|u_0\|_{L^2(\Omega)}^2\right) = \Re\left(\int_0^T [\mathrm{i}\bar{u}\partial_{\mathbf{n}} u]_{x_l}^{x_r}\,\mathrm{d}t\right) + \Re\left(\mathrm{i}\int_0^T\int_{x_l}^{x_r} V|u|^2\,\mathrm{d}x\,\mathrm{d}t\right). \tag{42}$$

Since V is a real-valued potential, the second term of the right-hand side of Eq. (42) is equal to zero. Therefore, we now have to study the sign of the first term. Let us focus on ABC_0^4, the case ABC_0^2 being then trivial. The quantity $i\bar{u}(x)\partial_{\mathbf{n}} u(x)$ is the sum of the two terms

$$-\mathrm{i}\mathrm{e}^{-\mathrm{i}\pi/4}\overline{\mathrm{e}^{-\mathrm{i}\nu}u}\partial_t^{1/2}\left(\mathrm{e}^{-\mathrm{i}\nu}u\right) \tag{43}$$

and

$$\frac{\mathrm{sg}(\partial_{\mathbf{n}}V)}{4}\overline{\sqrt{|\partial_{\mathbf{n}}V|}\mathrm{e}^{-\mathrm{i}\nu}u}\; I_t\Big(\sqrt{|\partial_{\mathbf{n}}V|}\mathrm{e}^{-\mathrm{i}\nu}u\Big). \tag{44}$$

Then, for $x = x_{\mathrm{l,r}}$, we have to determine the sign of the two quantities

$$\Re\Big(-\mathrm{i}\mathrm{e}^{-\mathrm{i}\pi/4}\int_0^T \overline{\varphi_{\mathrm{l,r}}(t)}\partial_t^{1/2}\varphi_{\mathrm{l,r}}(t)\mathrm{d}t\Big), \tag{45}$$

$$\Re\Big(\int_0^T \frac{\mathrm{sg}(\partial_{\mathbf{n}}V(x_{\mathrm{l,r}},t))}{4}\overline{\psi_{\mathrm{l,r}}(t)}I_t\psi_{\mathrm{l,r}}(t)\mathrm{d}t\Big), \tag{46}$$

with $\varphi_{\mathrm{l,r}}(t) = (\mathrm{e}^{-\mathrm{i}\nu}u)(x_{\mathrm{l,r}},t)$ and $\psi_{\mathrm{l,r}}(t) = (\sqrt{|\partial_{\mathbf{n}}V|}\mathrm{e}^{-\mathrm{i}\nu}u)(x_{\mathrm{l,r}},t)$. In the above relations, we set $f_{\mathrm{l,r}} = f(x_{\mathrm{l,r}})$, for a given function f. Thanks to Lemma 1, the term in (45) is negative. Under the assumption that the sign of $\partial_{\mathbf{n}}V(x_{\mathrm{l,r}},t)$ does not depend on the time t, one can isolate $\mathrm{sg}(\partial_{\mathbf{n}}V(x_{\mathrm{l,r}},t))$ out of the integral in (46) showing then that the integral term is equal to zero thanks to Lemma 1. This finally proves that the left-hand side of (42) is negative and that the energy inequality (40) holds. □

Remark 3. If V is a complex-valued potential [23], some results remain true under the assumption that V is dissipative, that is $\Im(V(x,t)) \geqslant 0$, for $(x,t) \in \mathbb{R}\times[0;T]$. More precisely, one can still construct the artificial boundary conditions ABC_0^M given by (36)–(38), with $M = 2, 4$. Moreover, the well-posedness result holds for ABC_0^2. It is still possible to symmetrize the artificial boundary condition ABC_0^4 by writing

$$\partial_{\mathbf{n}}V_{\mathrm{l,r}} = \mathrm{e}^{\mathrm{i}\theta_{\mathrm{l,r}}}\sqrt{|\partial_{\mathbf{n}}V_{\mathrm{l,r}}|}\sqrt{|\partial_{\mathbf{n}}V_{\mathrm{l,r}}|}, \tag{47}$$

where $t\mapsto\theta_{\mathrm{l,r}}(t)$ denotes the argument of $\partial_{\mathbf{n}}V$ on the boundary $x_{\mathrm{l,r}}$. However, the adaptation of the proof of the well-posedness result for the additional term does not seem possible even for a constant argument.

2.5. The other choice of ABC: ABC_1^M

After studying the first ABC, let us consider the other artificial boundary condition ABC_1^M, for $M = 2$ and $M = 4$.

Proposition 5. *For $\ell = 1$, the artificial boundary condition of order M based on the first strategy for symbols (24) is given by*

$$\partial_{\mathbf{n}}u + \Lambda_1^M u = 0, \quad \text{on } \Sigma_T, \tag{48}$$

with

$$\Lambda_1^2(x,t,\partial_t)u = Op\Big(-\mathrm{i}\sqrt{-\tau+V}\Big)u \tag{49}$$

and

$$\Lambda_1^4(x,t,\partial_t)u = \Lambda_1^2(x,t,\partial_t)u + \frac{1}{4}Op\Big(\frac{\partial_x V}{-\tau+V}\Big)u. \tag{50}$$

The boundary condition (48) is referred to as ABC_1^M in the sequel of the paper.

Studying the well-posedness of the initial boundary value problem related to the boundary condition ABC_1^M (48)–(50) is more difficult than ABC_0^M. Indeed, the expressions of the pseudodifferential operators involved in (49) and (50) is based on the inverse Fourier representation (10). Therefore, proving an equivalent result to Lemma 1 cannot be obtained by an argument based on the Plancherel Theorem for a general potential V depending on x and t. However, if $V(x,t) = V(x)$, then the well-posedness result is trivial since ABC_1^M is strictly equivalent to ABC_0^M. This is the aim of the next section.

2.6. The case $V = V(x)$: connection between the ABCs and numerical accuracy comparisons

Our goal here is to prove that ABC_0^M and ABC_1^M are equivalent if the potential does not depend on t. This is no longer true if V is also time-dependent (we will see a modified version of these operators for a suitable numerical approximation in Section 3.2). The result is mainly based on the following Lemma.

Lemma 2. *If a is a t-independent symbol of S^m and $V(x,t) = V(x)$, then the following identity holds:*

$$Op(a(\tau - V(x)))u = \mathrm{e}^{\mathrm{i}tV}Op(a(\tau))\big(\mathrm{e}^{-\mathrm{i}tV}u(x,t)\big). \tag{51}$$

Proof. Let us write the definition of the symbol as an inverse Fourier transform and let us make the change of variable $\rho = \tau - V(x)$ in the considered integral. Then, we have the following set of equalities:

$$\begin{aligned} Op(a(\tau - V(x)))u &= \int_{\mathbb{R}} a(\tau - V(x))\mathcal{F}_t(u)(x,\tau)\mathrm{e}^{\mathrm{i}t\tau}\,\mathrm{d}\tau \\ &= \int_{\mathbb{R}} a(\rho)\mathcal{F}_t(u)(x,\rho + V(x))\mathrm{e}^{\mathrm{i}t\rho}\mathrm{e}^{\mathrm{i}tV(x)}\,\mathrm{d}\rho \\ &= \mathrm{e}^{\mathrm{i}tV(x)}\int_{\mathbb{R}} a(\rho)\mathcal{F}_t\big(t\mapsto \mathrm{e}^{-\mathrm{i}tV(x)}u(x,t)\big)(x,\rho)\mathrm{e}^{\mathrm{i}t\rho}\,\mathrm{d}\rho \\ &= \mathrm{e}^{\mathrm{i}tV(x)}Op(a(\tau))(\mathrm{e}^{-\mathrm{i}tV(x)}u(x,t)), \end{aligned}$$

leading to the proof of the Lemma. □

A direct application of the above Lemma gives the following Corollary.

Corollary 2. *If the potential V is time independent, then the artificial boundary conditions ABC_0^M and ABC_1^M are equivalent, for $M = 2, 4$, with $\mathcal{V}(x,t) = tV(x)$. In particular, the well-posedness of the associated bounded initial value problem is immediate from Proposition 4.*

Proof. The proof is direct applying Lemma 2. □

Among the class of x-dependent potentials, some exact solutions are known (see e.g. [9]) since they can be related to the free-potential Schrödinger equation. It is in particular known that the following traveling Gaussian beam

$$u^\star(x,t) = \sqrt{\frac{\mathrm{i}}{-4t+\mathrm{i}}}\exp\left(\frac{-\mathrm{i}x^2 - k_0 x + k_0^2 t}{-4t+\mathrm{i}}\right) \tag{52}$$

is solution to (1) for $V = 0$ with suitable initial condition, where k_0 is the wavenumber. Then, if u is solution to (1) with the linear potential $V(x) = \alpha x$, $\alpha \in \mathbb{R}$, and $u_0 = u_0^\star$, it is given by the expression

$$u(x,t) = \mathrm{e}^{-\mathrm{i}\left(-\alpha t x + \frac{t^3}{3}|\alpha|^2\right)}u^\star(x - t^2\alpha, t). \tag{53}$$

(Other solutions can be constructed for both repulsive and attractive quadratic potentials [9].) Since the exact reference solution is known in this case for the gaussian beam, one can compute $\partial_{\mathbf{n}}u$ on the boundary of the computational domain, and compare it with $-\Lambda_0^M u$ to test the accuracy of ABC_0^M. To this aim, we fix $V(x) = x$ and $x_r = 5$. We present in Fig. 3 the evolution of the absolute error $|\partial_{\mathbf{n}}u + \Lambda_0^M u|$ (which should be equal to zero for a transparent boundary condition) at the right point x_r for various values of k_0 and on the time interval $[0;T]$, setting $T = 1.5$. It is computed from the exact operators representations (11) and (12) using a formal computer algebra system. For completeness, we also provide the results when the TBC of the Schrödinger equation without potential is used (see Eq. (3)). It is labelled "Without potential". We directly observe that the fourth-order ABC always gives a much better accuracy than the second-order one. The results with the "Without potential" TBC also lead to very large errors. Moreover, the difference increases when higher wavenumbers are considered, which is consistent with the *a priori* high-frequency asymptotic expansion (15).

3. Semi-discretization schemes and their properties

The aim of this section is to proceed to the semi-discretization in time of the artificial boundary conditions that we have previously developed. Let us first consider the boundary conditions ABC_0^M. According to Proposition 3, we have

$$ABC_0^2: \ \partial_{\mathbf{n}}u + \mathrm{e}^{-\mathrm{i}\pi/4}\mathrm{e}^{\mathrm{i}\nu}\partial_t^{1/2}\big(\mathrm{e}^{-\mathrm{i}\nu}u\big) = 0, \tag{54}$$

$$ABC_0^4: \ \partial_{\mathbf{n}}u + \mathrm{e}^{-\mathrm{i}\pi/4}\mathrm{e}^{\mathrm{i}\nu}\partial_t^{1/2}\big(\mathrm{e}^{-\mathrm{i}\nu}u\big) + \mathrm{i}\,\mathrm{sg}(\partial_{\mathbf{n}}V)\frac{\sqrt{|\partial_{\mathbf{n}}V|}}{2}\mathrm{e}^{\mathrm{i}\nu}I_t\left(\frac{\sqrt{|\partial_{\mathbf{n}}V|}}{2}\mathrm{e}^{-\mathrm{i}\nu}u\right) = 0. \tag{55}$$

We use the symmetrical form of ABC_0^4, which is a keypoint in the case $V = V(x,t)$. The associated initial boundary value problem is then

$$\begin{cases} \mathrm{i}\partial_t u + \partial_x^2 u + Vu = 0, \quad \text{in } \Omega_T, \\ \partial_{\mathbf{n}}u + \Lambda_0^M u = 0, \quad \text{on } \Sigma_T, \text{for } M = 2 \text{ or } 4, \\ u(\cdot,0) = u_0, \quad \text{in } \Omega, \end{cases} \tag{56}$$

for a maximal time of computation T.

Let us consider an interior Crank–Nicolson scheme for the time discretization of system (56). The interval $[0;T]$ is uniformly discretized using N intervals. Let $\Delta t = T/N$ be the time step and let us set $t_n = n\Delta t$. Furthermore, u^n stands for an approximation of $u(t_n)$ and $V^n = V(x,t_n)$. If $V = V(x)$ is a time-independent potential, then the Crank–Nicolson discretization of the Schrödinger equation is given by

$$\mathrm{i}\frac{u^{n+1} - u^n}{\Delta t} + \partial_x^2\left(\frac{u^{n+1} + u^n}{2}\right) + V\frac{u^{n+1} + u^n}{2} = 0, \quad \text{for } n = 0, \ldots, N-1. \tag{57}$$

If $V = V(x,t)$, for matters of symmetry, we choose the following time-discretization of the interior equation:

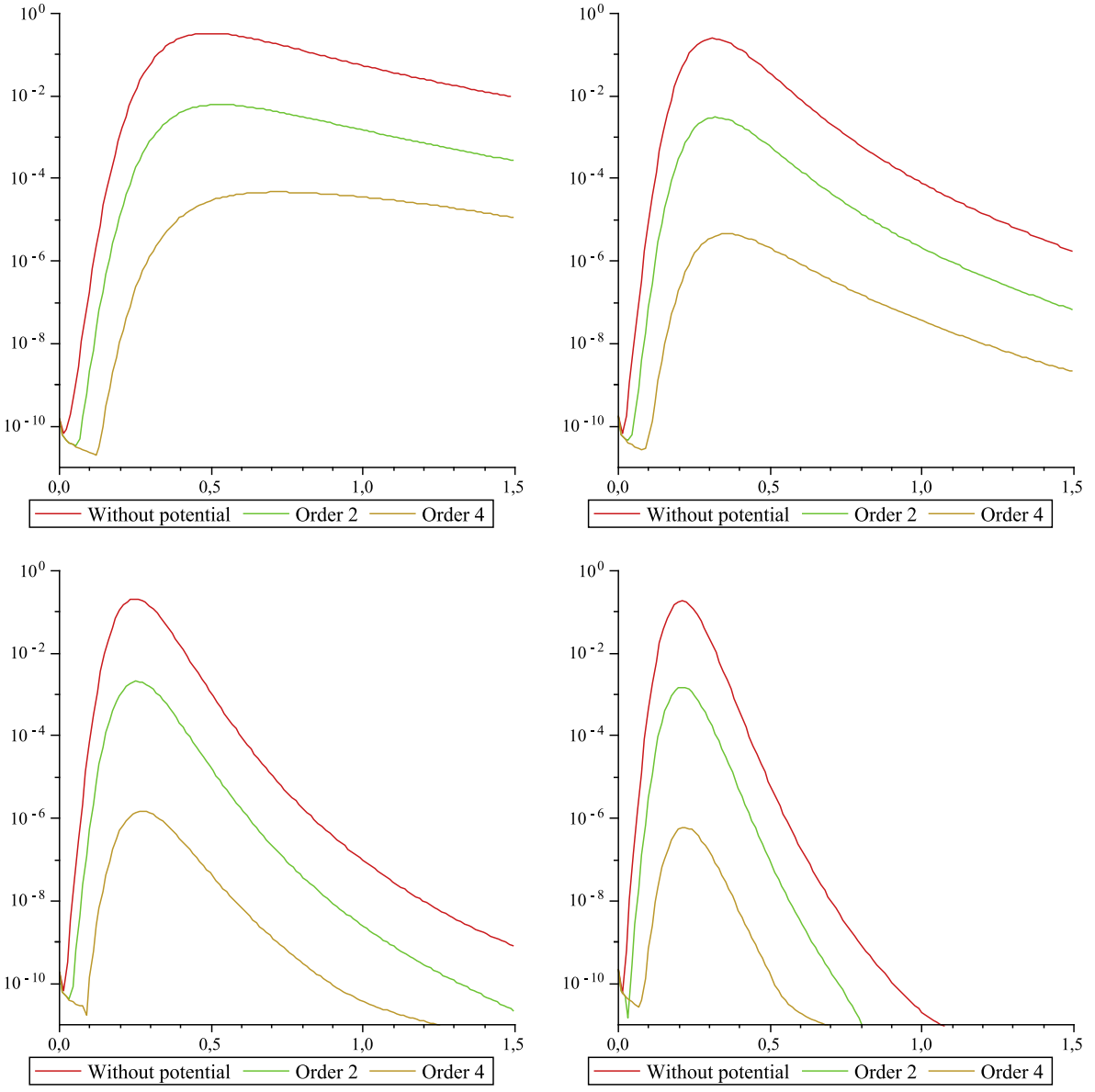

Fig. 3. Time variations of the absolute error $|\partial_{\mathbf{n}} u + \Lambda_0^M u|$ at $x_r = 5$, for $M = 2, 4$, and for the "Without potential" ABC, for the exact reference solution. The potential is $V(x,t) = x$ and we consider four values of k_0 (top, left: $k_0 = 5$; top, right: $k_0 = 8$; bottom, left: $k_0 = 10$; bottom, right: $k_0 = 12$).

$$\mathrm{i}\frac{u^{n+1}-u^n}{\Delta t} + \partial_x^2 \frac{u^{n+1}+u^n}{2} + \frac{V^{n+1}+V^n}{2}\frac{u^{n+1}+u^n}{2} = 0. \tag{58}$$

Another possible discretization could be

$$\mathrm{i}\frac{u^{n+1}-u^n}{\Delta t} + \partial_x^2 \frac{u^{n+1}+u^n}{2} + \frac{V^{n+1}u^{n+1}+V^n u^n}{2} = 0. \tag{59}$$

Nevertheless, this discretization does not preserve the symmetry of the interior equation. As a consequence, we are unable to prove a stability result (for discrete convolutions) with this discretization. Thus, we will treat only the discretization given by (58) where unconditional stability can be obtained.

Let us remark that, for implementation issues, it is often useful to set $v^{n+1} = \frac{u^{n+1}+u^n}{2} = u^{n+1/2}$, with $u^{-1} = 0$ and $u^0 = u_0$. Similarly, we set $W^{n+1} = \frac{V^{n+1}+V^n}{2} = V^{n+1/2}$. Then, the time scheme (58) reads

$$2\mathrm{i}\frac{v^{n+1}}{\Delta t} + \partial_x^2 v^{n+1} + W^{n+1}v^{n+1} = 2\mathrm{i}\frac{u^n}{\Delta t}. \tag{60}$$

It is well-known that a discretization of the TBC (3) which preserves the stability of the Crank–Nicolson scheme for the free-potential Schrödinger equation is not a trivial task. We propose here two solutions for the discretization of the ABCs that we propose. The first one is based on semi-discrete convolutions for the fractional operators involved in (54) and (55). We are then able to show that the resulting semi-discrete scheme is unconditionally stable. At the same time, a solution based on convolution operators may require long computational times. The second solution that we study is based on the approximation of the fractional operators through the solution of auxiliary differential equations which can be solved explicitly. The evaluation is then extremely efficient but at the same time, no stability proof is at hand.

3.1. Discretization based on discrete convolutions

Let us first recall that if $(f_n)_{n\in\mathbb{N}}$ is a given sequence of complex values, we denote by $\mathcal{Z}(f_n)$ or $\hat{f}$ the complex-valued function defined for $|z| \geqslant R(\mathcal{Z}(f_n))$ by the series

$$\hat{f}(z) = \mathcal{Z}(f_n)(z) = \sum_{n=0}^{+\infty} f_n z^{-n},$$

where $R(\mathcal{Z}(f_n))$ is the convergence radius of the series. Then, we have the following proposition (see e.g. [4,6]).

Proposition 6. *If $\{f^n\}_{n\in\mathbb{N}}$ is a sequence of complex numbers approximating $\{f(t_n)\}_{n\in\mathbb{N}}$, then the approximations of $\partial_t^{1/2} f(t_n)$, $I_t^{1/2} f(t_n)$ and $I_t f(t_n)$ with respect to the Crank–Nicolson scheme for a time step Δt are given by the numerical quadrature formulas*

$$\partial_t^{1/2} f(t_n) \approx \sqrt{\frac{2}{\Delta t}} \sum_{k=0}^{n} \beta_{n-k} f^k, \tag{61}$$

$$I_t^{1/2} f(t_n) \approx \sqrt{\frac{\Delta t}{2}} \sum_{k=0}^{n} \alpha_{n-k} f^k, \tag{62}$$

$$I_t f(t_n) \approx \frac{\Delta t}{2} \sum_{k=0}^{n} \gamma_{n-k} f^k, \tag{63}$$

where the sequences $(\alpha_n)_{n\in\mathbb{N}}$, $(\beta_n)_{n\in\mathbb{N}}$ and $(\gamma_n)_{n\in\mathbb{N}}$ are such that

$$\begin{cases} (\alpha_0, \alpha_1, \alpha_2, \alpha_3, \alpha_4, \alpha_5, \ldots) = \left(1, 1, \frac{1}{2}, \frac{1}{2}, \frac{3}{8}, \frac{3}{8}, \ldots\right), \\ \beta_k = (-1)^k \alpha_k, \quad \forall k \geqslant 0, \\ (\gamma_0, \gamma_1, \gamma_2, \gamma_3, \ldots) = (1, 2, 2, \ldots). \end{cases} \tag{64}$$

Moreover, their respective $\mathcal{Z}$-transforms are given by

$$\mathcal{Z}(\alpha_n)(z) = \mathrm{i}\sqrt{\frac{1+z}{1-z}}, \quad \mathcal{Z}(\beta_n)(z) = -\mathrm{i}\sqrt{\frac{1-z}{1+z}}, \quad \mathcal{Z}(\gamma_n)(z) = -\frac{1+z}{1-z}, \tag{65}$$

for $|z| > 1$.

Remark 4. Let us remark that analytical formulae for (64) are also given in [25].

The weak formulation of (58) writes, for $\psi \in L^2(\Omega)$

$$\frac{2\mathrm{i}}{\Delta t} \int_{x_\mathrm{l}}^{x_\mathrm{r}} (v^{n+1} - u^n)\psi \,\mathrm{d}x + \left[\partial_x v^{n+1} \psi\right]_{x_\mathrm{l}}^{x_\mathrm{r}} - \int_{x_\mathrm{l}}^{x_\mathrm{r}} \partial_x v^{n+1} \partial_x \psi \,\mathrm{d}x + \int_{x_\mathrm{l}}^{x_\mathrm{r}} W^{n+1} v^{n+1} \psi \,\mathrm{d}x = 0. \tag{66}$$

According to the interior scheme (58), the semi-discretization of ABC_0^2 for v at time t_{n+1} is

$$\partial_{\mathbf{n}} v^{n+1}(x_{\mathrm{l,r}}) = -\mathrm{e}^{-\mathrm{i}\pi/4} \mathrm{e}^{\mathrm{i}\mathcal{W}^{n+1}} \sqrt{\frac{2}{\Delta t}} \sum_{k=0}^{n+1} \beta_{n+1-k} \mathrm{e}^{-\mathrm{i}\mathcal{W}^k} v^k(x_{\mathrm{l,r}})$$

and for ABC_0^4

$$\begin{aligned} \partial_{\mathbf{n}} v^{n+1}(x_{\mathrm{l,r}}) = & -\mathrm{e}^{-\mathrm{i}\pi/4} \mathrm{e}^{\mathrm{i}\mathcal{W}^{n+1}} \sqrt{\frac{2}{\Delta t}} \sum_{k=0}^{n+1} \beta_{n+1-k} \mathrm{e}^{-\mathrm{i}\mathcal{W}^k} v^k(x_{\mathrm{l,r}}) \\ & - \mathrm{i}\,\mathrm{sg}(\partial_{\mathbf{n}} W^{n+1}) \frac{\sqrt{|\partial_{\mathbf{n}} W^{n+1}|}}{2} \mathrm{e}^{\mathrm{i}\mathcal{W}^{n+1}} \frac{\Delta t}{2} \sum_{k=0}^{n+1} \gamma_{n+1-k} \frac{\sqrt{|\partial_{\mathbf{n}} W^k|}}{2} \mathrm{e}^{-\mathrm{i}\mathcal{W}^k} v^k(x_{\mathrm{l,r}}), \end{aligned}$$

with the notation $\mathcal{W}^{n+1} = \frac{\nu^{n+1}+\nu^n}{2}$. Then, we have the following proposition:

Proposition 7. *The semi-discrete Crank–Nicolson scheme for the initial boundary value problem (56) is given by*

$$\begin{cases} 2\mathrm{i}\frac{v^{n+1}-u^n}{\Delta t}+\partial_x^2 v^{n+1}+W^{n+1}v^{n+1}=0, \quad \text{in } \Omega \\ \partial_{\mathbf{n}} v^{n+1}+\Lambda_0^{M,n+1}v^{n+1}=0, \quad \text{on } \Sigma, \quad \text{for } M=2 \text{ or } 4, \\ u^0=u_0, \quad \text{in } \Omega, \end{cases} \tag{67}$$

for $n=0,\dots,N-1$, where $v^{n+1}=\frac{u^{n+1}+u^n}{2}$, $W^{n+1}=\frac{\mathcal{V}^{n+1}+\mathcal{V}^n}{2}$, and where the semi-discrete operators $\Lambda_0^{2,n+1}$, $\Lambda_0^{4,n+1}$ are defined by

$$\Lambda_0^{2,n+1}v^{n+1}=\mathrm{e}^{-\mathrm{i}\pi/4}\mathrm{e}^{\mathrm{i}\mathcal{W}^{n+1}}\sqrt{\frac{2}{\Delta t}}\sum_{k=0}^{n+1}\beta_{n+1-k}\mathrm{e}^{-\mathrm{i}\mathcal{W}^k}v^k, \tag{68}$$

$$\Lambda_0^{4,n+1}v^{n+1}=\Lambda_0^{2,n+1}v^{n+1}+\mathrm{i}\,\mathrm{sg}(\partial_{\mathbf{n}}W^{n+1})\frac{\sqrt{|\partial_{\mathbf{n}}W^{n+1}|}}{2}\mathrm{e}^{\mathrm{i}\mathcal{W}^{n+1}}\frac{\Delta t}{2}\sum_{k=0}^{n+1}\gamma_{n+1-k}\frac{\sqrt{|\partial_{\mathbf{n}}W^k|}}{2}\mathrm{e}^{-\mathrm{i}\mathcal{W}^k}v^k. \tag{69}$$

Here, $\mathcal{W}^{n+1}$ is defined by $\mathcal{W}^{n+1}=\frac{\mathcal{V}^{n+1}+\mathcal{V}^n}{2}$, $\mathcal{V}^n(x)$ being the approximation of $\mathcal{V}(x,t_n)$ using the trapezoidal rule 63 ($\mathcal{V}$ is given by (7)). Moreover, for $M=2$, one has the following energy inequality:

$$\forall n\in\{0,\dots,N\}, \quad \|u^n\|_{L^2(\Omega)}\leqslant\|u^0\|_{L^2(\Omega)} \tag{70}$$

and if $\mathrm{sg}(\partial_{\mathbf{n}}W^k)$ is constant, then (70) also holds for $M=4$. This proves the $L^2(\Omega)$ stability of the scheme. Inequality (70) is the semi-discrete version of (40) under the corresponding assumptions.

Proof. Let us multiply the first equation of (67) by $-\mathrm{i}\overline{v^{p+1}}$ and integrate by parts on Ω. This gives, for $p\geqslant 0$,

$$\int_\Omega\frac{|u^{p+1}|^2-|u^p|^2+\mathrm{i}\Im(u^{p+1}\overline{u^p})}{2\Delta t}\mathrm{d}x-\mathrm{i}\left[\overline{v^{p+1}}\partial_x v^{p+1}\right]_{x_\mathrm{l}}^{x_\mathrm{r}}+\mathrm{i}\int_\Omega|\partial_x v^{p+1}|^2\mathrm{d}x-\mathrm{i}\int_\Omega W^{p+1}|v^{p+1}|^2\mathrm{d}x=0.$$

Since V is assumed to be real, taking the real part of this expression yields

$$\frac{1}{\Delta t}\frac{\|u^{p+1}\|_{L^2(\Omega)}^2-\|u^p\|_{L^2(\Omega)}^2}{2}=\Re\left(\mathrm{i}\left[\overline{v^{p+1}}\partial_x v^{p+1}\right]_{x_\mathrm{l}}^{x_\mathrm{r}}\right).$$

Summing up the terms in the above equation from $p=0$ to $p=n-1$, we obtain

$$\frac{1}{2\Delta t}\left(\|u^n\|_{L^2(\Omega)}^2-\|u^0\|_{L^2(\Omega)}^2\right)=\Re\left(\sum_{p=0}^{n-1}\mathrm{i}\left[\overline{v^{p+1}}\partial_x v^{p+1}\right]_{x_\mathrm{l}}^{x_\mathrm{r}}\right)=\sum_{\gamma=l,r}A_\gamma, \tag{71}$$

with

$$A_\gamma=\Re\left(\sum_{p=0}^{n-1}\mathrm{i}\overline{v^{p+1}(x_\gamma)}\partial_{\mathbf{n}}v^{p+1}(x_\gamma)\right) \quad \text{for } \gamma=l,r. \tag{72}$$

Let us focus on the right endpoint x_r, the left endpoint x_l can be treated similarly. We get

$$\begin{aligned}\mathrm{i}\overline{v^{p+1}}(x_\mathrm{r})\partial_{\mathbf{n}}v^{p+1}(x_\mathrm{r})=&-\mathrm{i}\mathrm{e}^{-\mathrm{i}\pi/4}\sqrt{\frac{2}{\Delta t}}\mathrm{e}^{\mathrm{i}\mathcal{W}_\mathrm{r}^{p+1}}\overline{v_\mathrm{r}^{p+1}}\sum_{k=0}^{p+1}\beta_{p+1-k}\mathrm{e}^{-\mathrm{i}\mathcal{W}_\mathrm{r}^k}v_\mathrm{r}^k\\&+\mathrm{sg}(\partial_{\mathbf{n}}W_\mathrm{r}^{p+1})\frac{\Delta t}{2}\frac{\sqrt{|\partial_{\mathbf{n}}W_\mathrm{r}^{p+1}|}}{2}\mathrm{e}^{\mathrm{i}\mathcal{W}^{p+1}}\overline{v_\mathrm{r}^{p+1}}\sum_{k=0}^{p+1}\gamma_{p+1-k}\frac{\sqrt{|\partial_{\mathbf{n}}W_\mathrm{r}^k|}}{2}\mathrm{e}^{-\mathrm{i}\mathcal{W}_\mathrm{r}^k}v_\mathrm{r}^k\end{aligned}$$

that is

$$\sum_{p=0}^{n-1}\mathrm{i}\overline{v^{p+1}}(x_\mathrm{r})\partial_{\mathbf{n}}v^{p+1}(x_\mathrm{r})=-\mathrm{i}\mathrm{e}^{-\mathrm{i}\pi/4}\sqrt{\frac{2}{\Delta t}}\sum_{p=0}^{n-1}\overline{\chi_\mathrm{r}^{p+1}}\sum_{k=0}^{p+1}\beta_{p+1-k}\chi_\mathrm{r}^k+\mathrm{sg}(\partial_{\mathbf{n}}W_\mathrm{r})\frac{\Delta t}{2}\sum_{p=0}^{n-1}\overline{\psi_\mathrm{r}^{p+1}}\sum_{k=0}^{p+1}\gamma_{p+1-k}\psi_\mathrm{r}^k, \tag{73}$$

with $\chi_\mathrm{r}^k=\mathrm{e}^{-\mathrm{i}\mathcal{W}_\mathrm{r}^k}v_\mathrm{r}^k$, $\psi_\mathrm{r}^k=\frac{\sqrt{|\partial_{\mathbf{n}}W_\mathrm{r}^k|}}{2}\mathrm{e}^{-\mathrm{i}\mathcal{W}_\mathrm{r}^k}v_\mathrm{r}^k$, $\mathcal{W}_\mathrm{r}^k=\mathcal{W}^k(x_\mathrm{r})$ and $W_\mathrm{r}^k=W^k(x_\mathrm{r})$. The assumption that $\mathrm{sg}(\partial_{\mathbf{n}}W_\mathrm{r}^k)$ is constant is fundamental here. This implies that the study of the second term of the right-hand side of (73) reduces to the study of a symmetrical term similar to the first term of the right-hand side. To determine the sign of the real part of the two terms in the right-hand side of (73), we use the following Lemma. □

Lemma 3. *Let $(\beta_n)_n$ and $(\gamma_n)_n$ be the sequences defined in (64). Let $(\varphi^k)_{k\in\mathbb{N}}$ be a complex valued sequence such that $R_\varphi<1$. Then, we have the following properties*

$$Q_\beta=\mathrm{e}^{-\mathrm{i}\pi/4}\sum_{p=0}^{n-1}\overline{\varphi^{p+1}}\sum_{k=0}^{p+1}\beta_{p+1-k}\varphi^k\in\mathbb{R}^-\cup\mathrm{i}\mathbb{R}^- \tag{74}$$

and

$$Q_\gamma = \sum_{p=0}^{n-1} \overline{\varphi^{p+1}} \sum_{k=0}^{p+1} \gamma_{p+1-k} \varphi^k \in i\mathbb{R}. \tag{75}$$

This result immediately shows that the real part of the first term in the right-hand side of (73) is negative, whereas the second term is purely imaginary. Finally, the inequality (70) holds, ending hence the proof of Proposition 7.

Let us prove now Lemma 3.

Proof. [Proof of Lemma 3]. Another way of writing Q_β is given by

$$Q_\beta = \sum_{p=0}^{n-1} \left(\overline{\varphi^{p+1}} \sum_{k=0}^{p+1} \beta_{p+1-k} \varphi^k \right) = \sum_{p=0}^{n-1} \overline{\varphi^{p+1}} \left(\beta_k \star \varphi^k\right)_{p+1} = \sum_{p=0}^{+\infty} \overline{\phi_{p+1}^n} \left(\beta_k \star \phi_k^n\right)_{p+1},$$

where we have extended $(\varphi^k)_{0\leqslant k\leqslant n}$ to an infinite sequence $(\phi_k^n)_{k\in\mathbb{N}}$ by

$$\phi_k^n = \begin{cases} \varphi^k & \text{if } k \leqslant n, \\ (-1)^j \varphi^n & \text{if } k = n+j, \text{with } j > 0. \end{cases} \tag{76}$$

We recall the Plancherel theorem [11].

Lemma 4.
Let us consider two sequences $(f_p)_{p\in\mathbb{N}}$ and $(g_p)_{p\in\mathbb{N}}$. If $R_{\hat f} R_{\hat g} < 1$, then $\mathcal{Z}(\overline{f_p} g_p)$ exists for $|z| > R_{\hat f} R_{\hat g}$ and we have

$$\sum_{p=0}^{+\infty} \overline{f_p} g_p = \mathcal{Z}\left(\overline{f_p} g_p\right)(z=1) = \frac{1}{2\pi} \int_0^{2\pi} \overline{\hat f(r\mathrm{e}^{\mathrm{i}\theta})} \hat g\left(\frac{\mathrm{e}^{\mathrm{i}\theta}}{r}\right) \mathrm{d}\theta, \tag{77}$$

where the integration path is a circle with radius r such that $R_{\hat f} < r < 1/R_{\hat g}$. Moreover, if the two radii satisfy $R_{\hat f} < 1$ and $R_{\hat g} < 1$, then $r = 1$ can be chosen in (77).

Applying Lemma 4, we have

$$Q_\beta = \mathcal{Z}\left(\overline{\phi_{p+1}^n} \left(\beta_k \star \phi_k^n\right)_{p+1}\right)(z=1) = \frac{1}{2\pi} \int_0^{2\pi} \overline{\hat f(\mathrm{e}^{\mathrm{i}\theta})} \hat g(\mathrm{e}^{\mathrm{i}\theta}) \mathrm{d}\theta.$$

Using the shifting and convolution theorems (see e.g. [11]), we obtain

$$\hat f(z) = \mathcal{Z}(\phi_{p+1}^n)(z) = \frac{z+1}{2} \hat\varphi(z),$$

$$\hat g(z) = \mathcal{Z}\left(\left(\beta_k \star \phi_k^n\right)_{p+1}\right)(z) = \frac{z+1}{2} \mathcal{Z}\left(\left(\beta_k \star \phi_k^n\right)_p\right)(z) = \frac{z+1}{2} \mathcal{Z}(\beta_k)(z) \hat\varphi(z),$$

with $\hat\varphi(z) = \mathcal{Z}(\varphi^k)(z)$. Hence, a new expression of Q_β is obtained as

$$Q_\beta = -\frac{\mathrm{i}}{2\pi} \int_0^{2\pi} \left\{ \left|\frac{z+1}{2}\right|^2 |\hat\varphi(z)|^2 \sqrt{\frac{1-z}{1+z}} \right\}\Bigg|_{z=\mathrm{e}^{\mathrm{i}\theta}} \mathrm{d}\theta.$$

Moreover, since $z \mapsto \frac{1-z}{1+z}$ maps $\mathcal{C}(0,1)$ to $\mathrm{i}\mathbb{R}$, the application $z \mapsto -\mathrm{i}\mathrm{e}^{-\mathrm{i}\pi/4} \sqrt{\frac{1-z}{1+z}}$ transforms $\mathcal{C}(0,1)$ to $\mathbb{R}^- \cup \mathrm{i}\mathbb{R}^-$, proving relation (74). Similarly, we have for Q_γ

$$\begin{aligned} Q_\gamma &= \frac{1}{2\pi} \int_0^{2\pi} \left\{ \left|\frac{z+1}{2}\right|^2 |\hat\varphi(z)|^2 \mathcal{Z}(\gamma_n)(z) \right\}\Bigg|_{z=\mathrm{e}^{\mathrm{i}\theta}} \mathrm{d}\theta \\ &= -\frac{1}{2\pi} \int_0^{2\pi} \left\{ \left|\frac{z+1}{2}\right|^2 |\hat\varphi(z)|^2 \frac{1+z}{1-z} \right\}\Bigg|_{z=\mathrm{e}^{\mathrm{i}\theta}} \mathrm{d}\theta. \end{aligned}$$

This implies that $Q_\gamma \in i\mathbb{R}$ since the image of $\mathcal{C}(0,1)$ is $i\mathbb{R}$ by $z \mapsto \frac{1+z}{1-z}$. This finally proves relation (75) and completes the proof of Lemma 3. □

3.2. Discretization based on auxiliary functions

While the previous strategy based on discrete convolution operators seems accurate and provides a stability result, it may lead to significantly long computational times. Moreover, we will see during the numerical simulations that very small time steps Δt are required to attain the optimal accuracy of the artificial boundary conditions based on convolution operators. This can be relaxed using the following approach.

We saw that the ABC_0^M and ABC_1^M boundary conditions are equivalent in the case of time independent potentials. This is no longer true for a time dependent function V. In such a situation, the scheme developed above can be used for ABC_0^M. For ABC_1^M,

the discretizations of the resulting pseudodifferential operators involved is not easy to obtain. In particular, the operators with square-root symbols cannot be expressed in terms of fractional time operators since Lemma 2 does not hold. For these reasons, we introduce the following additional approximations.

Lemma 5. *The two following approximations hold*

$$Op\left(\sqrt{-\tau+V}\right)=\sqrt{\mathrm{i}\partial_t+V}\quad \mathrm{mod}(\mathrm{OPS}^{-3/2}) \tag{78}$$

and

$$Op\left(\frac{\partial_x V}{4}\frac{1}{-\tau+V}\right)=\mathrm{sg}(\partial_{\mathbf{n}}V)\frac{\sqrt{|\partial_{\mathbf{n}}V|}}{2}(\mathrm{i}\partial_t+V)^{-1}\frac{\sqrt{|\partial_{\mathbf{n}}V|}}{2}\quad \mathrm{mod}(\mathrm{OPS}^{-3}) \tag{79}$$

Proof. Let us set $A=\sqrt{\mathrm{i}\partial_t+V}$. The operator A is of order $1/2$ and its total symbol σ_A admits thus an expansion under the form: $\sigma_A\sim\sum_{\ell=0}^{+\infty}\sigma_{A,1/2-\ell/2}$. Since $A^2=i\partial_t+V$, we have

$$\sigma(A^2)=\sigma(\mathrm{i}\partial_t+V)=-\tau+V\sim\sum_{\alpha=0}^{+\infty}\frac{(-\mathrm{i})^\alpha}{\alpha!}\partial_\tau^\alpha\sigma_A\partial_t^\alpha\sigma_A. \tag{80}$$

Using the asymptotic expansion of σ_A and an identification of the same order terms in (80), we obtain the following approximation:

$$\sigma_A=\sigma(\sqrt{\mathrm{i}\partial_t+V})=\sqrt{-\tau+V}-\frac{\mathrm{i}}{8}\frac{\partial_t V}{\sqrt{-\tau+V^3}}\quad \mathrm{mod}(\mathrm{S}^{-5/2}).$$

In terms of operators, this gives relation (78).

Similarly, setting $B=(i\partial_t+V)^{-1}$, $B^{-1}=i\partial_t+V$ and writing $\sigma(BB^{-1})=1$, we get the asymptotic expansion

$$\sigma(\mathrm{i}\partial_t+V)^{-1}=\frac{1}{-\tau+V}+\frac{\mathrm{i}\partial_t V}{(-\tau+V)^3}\quad \mathrm{mod}(\mathrm{S}^{-4}). \tag{81}$$

If $\sigma_p(P)$ designates the principal symbol of a pseudodifferential operator P, the following set of equalities holds:

$$\begin{aligned}\sigma_p\left(\mathrm{sg}(\partial_{\mathbf{n}}V)\frac{\sqrt{|\partial_{\mathbf{n}}V|}}{2}(\mathrm{i}\partial_t+V)^{-1}\frac{\sqrt{|\partial_{\mathbf{n}}V|}}{2}\right) &= \mathrm{sg}(\partial_{\mathbf{n}}V)\frac{|\partial_{\mathbf{n}}V|}{4}\sigma_p(\mathrm{i}\partial_t+V)^{-1}\\ &= \frac{\partial_{\mathbf{n}}V}{4}\frac{1}{-\tau+V}.\end{aligned} \tag{82}$$

Combining (81) and (82), we obtain (79) at the operators level. □

Thanks to Lemma 5, we now define the new approximations of ABC_1^M (see Proposition 5)

$$\widetilde{\mathrm{ABC}_1^2}:\ \partial_{\mathbf{n}}u-\mathrm{i}\sqrt{\mathrm{i}\partial_t+V}u=0, \tag{83}$$

$$\widetilde{\mathrm{ABC}_1^4}:\ \partial_{\mathbf{n}}u-\mathrm{i}\sqrt{\mathrm{i}\partial_t+V}u+\mathrm{sg}(\partial_{\mathbf{n}}V)\frac{\sqrt{|\partial_{\mathbf{n}}V|}}{2}(\mathrm{i}\partial_t+V)^{-1}\left(\frac{\sqrt{|\partial_{\mathbf{n}}V|}}{2}u\right)=0. \tag{84}$$

Let us begin by the second-order condition (83). An alternative approach to discrete convolutions (which cannot be applied here) consists in approximating the square-root operator $\sqrt{\mathrm{i}\partial_t+V}$ using rational functions like in the present paper the mth order Padé approximants [22]

$$\sqrt{z}\approx R_m(z)=a_0^m+\sum_{k=1}^m\frac{a_k^m z}{z+d_k^m}=\sum_{k=0}^m a_k^m-\sum_{k=1}^m\frac{a_k^m d_k^m}{z+d_k^m}, \tag{85}$$

where the coefficients $(a_k^m)_{0\leqslant k\leqslant m}$ and $(d_k^m)_{1\leqslant k\leqslant m}$ are given by

$$a_0^m=0,\quad a_k^m=\frac{1}{m\cos^2\left(\frac{(2k+1)\pi}{4m}\right)},\quad d_k^m=\tan^2\left(\frac{(2k+1)\pi}{4m}\right). \tag{86}$$

Formally, $\sqrt{\mathrm{i}\partial_t+V}$ is approximated by

$$R_m(\mathrm{i}\partial_t+V)=\sum_{k=0}^m a_k^m-\sum_{k=1}^m a_k^m d_k^m(\mathrm{i}\partial_t+V+d_k^m)^{-1}. \tag{87}$$

Applying this process to Eq. (83), we have the new relation

$$\partial_{\mathbf{n}}u-\mathrm{i}\sum_{k=0}^m a_k^m u+\mathrm{i}\sum_{k=1}^m a_k^m d_k^m(\mathrm{i}\partial_t+V+d_k^m)^{-1}u=0, \tag{88}$$

which defines a second-order artificial boundary condition referred to as $\mathrm{ABC}^2_{1,m}$ in the sequel. To write a suitable form of the equation in view of an efficient numerical treatment, we classically introduce m auxiliary functions φ_k, for $1 \leqslant k \leqslant m$ (see Lindmann [19]) as follows:

$$\varphi_k = \left(\mathrm{i}\partial_t + V + d_k^m\right)^{-1} u \tag{89}$$

leading to the following equation:

$$\mathrm{i}\partial_t \varphi_k + (V + d_k^m)\varphi_k = u, \quad \text{for } 1 \leqslant k \leqslant m \text{ at } x = x_{\mathrm{l,r}}, \tag{90}$$

with the initial condition $\varphi_k(x,0) = 0$. The corresponding full artificial boundary condition is written as a system

$$\begin{cases} \partial_{\mathbf{n}} u - \mathrm{i}\sum\limits_{k=0}^{m} a_k^m u + \mathrm{i}\sum\limits_{k=1}^{m} a_k^m d_k^m \varphi_k = 0, \\ \mathrm{i}\partial_t \varphi_k + (V + d_k^m)\varphi_k = u, \qquad\qquad \text{for } 1 \leqslant k \leqslant m,\ x = x_{\mathrm{l,r}}, \\ \varphi_k(x,0) = 0. \end{cases} \tag{91}$$

Now, we have to discretize the above system. The semi-discretization of the interior scheme remains the same as before (58), and consequently, (91) becomes

$$\begin{cases} \partial_{\mathbf{n}} u^{n+1/2} - \mathrm{i}\sum\limits_{k=0}^{m} a_k^m u^{n+1/2} + \mathrm{i}\sum\limits_{k=1}^{m} a_k^m d_k^m \varphi_k^{n+1/2} = 0, \\ \mathrm{i}\frac{\varphi_k^{n+1} - \varphi_k^n}{\Delta t} + (V^{n+1/2} + d_k^m)\varphi_k^{n+1/2} = u^{n+1/2}, \\ \varphi_k^0 = 0, \end{cases} \tag{92}$$

for $1 \leqslant k \leqslant m$ and $x = x_{\mathrm{l,r}}$, that is, in terms of v^n functions

$$\begin{cases} \partial_{\mathbf{n}} v^{n+1} - \mathrm{i}\sum\limits_{k=0}^{m} a_k^m v^{n+1} + \mathrm{i}\sum\limits_{k=1}^{m} a_k^m d_k^m \varphi_k^{n+1/2} = 0, \\ \mathrm{i}\frac{\varphi_k^{n+1} - \varphi_k^n}{\Delta t} + (W^{n+1} + d_k^m)\varphi_k^{n+1/2} = v^{n+1}, \\ \varphi_k^0 = 0. \end{cases} \tag{93}$$

The auxiliary function φ_k^{n+1} can be easily expressed at point $x_{\mathrm{l,r}}$ as

$$\varphi_k^{n+1}(x_{\mathrm{l,r}}) = \frac{\frac{\mathrm{i}}{\Delta t} - \frac{W_{\mathrm{l,r}}^{n+1} + d_k^m}{2}}{\frac{\mathrm{i}}{\Delta t} + \frac{W_{\mathrm{l,r}}^{n+1} + d_k^m}{2}} \varphi_k^n(x_{\mathrm{l,r}}) + \frac{1}{\frac{\mathrm{i}}{\Delta t} + \frac{W_{\mathrm{l,r}}^{n+1} + d_k^m}{2}} v^{n+1}(x_{\mathrm{l,r}}). \tag{94}$$

Using the first equation of (93), we finally obtain

$$\partial_{\mathbf{n}} v^{n+1}(x_{\mathrm{l,r}}) + \left[-\mathrm{i}\sum_{k=0}^{m} a_k^m + \frac{\mathrm{i}}{2}\sum_{k=1}^{m} a_k^m d_k^m \frac{1}{\frac{\mathrm{i}}{\Delta t} + \frac{W_{\mathrm{l,r}}^{n+1} + d_k^m}{2}}\right] v^{n+1}(x_{\mathrm{l,r}}) = -\mathrm{i}\sum_{k=1}^{m} a_k^m d_k^m \frac{\frac{2\mathrm{i}}{\Delta t}}{\frac{\mathrm{i}}{\Delta t} + \frac{W_{\mathrm{l,r}}^{n+1} + d_k^m}{2}} \frac{\varphi_k^n(x_{\mathrm{l,r}})}{2}. \tag{95}$$

Eq. (95) finally gives a local inhomogeneous Fourier–Robin-type ABC, where the right-hand side is updated using (94).

Now, let us consider the fourth-order condition ABC_1^4 given by (84)

$$\partial_{\mathbf{n}} u - \mathrm{i}\sqrt{\mathrm{i}\partial_t + V}\, u + \mathrm{sg}(\partial_{\mathbf{n}} V)\frac{\sqrt{|\partial_{\mathbf{n}} V|}}{2}(\mathrm{i}\partial_t + V)^{-1}\left(\frac{\sqrt{|\partial_{\mathbf{n}} V|}}{2} u\right) \quad \text{on } \Sigma \times \mathbb{R}. \tag{96}$$

Then, one has to introduce one more additional auxiliary function ψ such that

$$(\mathrm{i}\partial_t + V)\psi = \frac{\sqrt{|\partial_{\mathbf{n}} V|}}{2} u. \tag{97}$$

We call $\mathrm{ABC}_{1,m}^4$ the resulting approximation of $\widetilde{\mathrm{ABC}_1^4}$ using the Padé approximation (85) and the additional differential equation (97). Using again a Crank–Nicolson discretization of ψ, one gets the following approximate representation of $\mathrm{ABC}_{1,m}^4$:

$$
\begin{cases}
\partial_{\mathbf{n}} v^{n+1}(x_{\mathrm{l,r}}) + \left[-\mathrm{i}\sum_{k=0}^{m} a_k^m + \frac{\mathrm{i}}{2}\sum_{k=1}^{m} a_k^m d_k^m \frac{1}{\frac{\mathrm{i}}{\Delta t}+\frac{W_{\mathrm{l,r}}^{n+1}+d_k^m}{2}} + \frac{1}{2}\mathrm{sg}(\partial_{\mathbf{n}} W_{\mathrm{l,r}}^{n+1}) \frac{\sqrt{|\partial_{\mathbf{n}} W_{\mathrm{l,r}}^{n+1}|}}{2} \frac{\sqrt{|\partial_{\mathbf{n}} W_{\mathrm{l,r}}^{n+1}|}}{\frac{\mathrm{i}}{\Delta t}+\frac{W_{\mathrm{l,r}}^{n+1}}{2}} \right] v^{n+1}(x_{\mathrm{l,r}}) \\
\quad = -\mathrm{i}\sum_{k=1}^{m} a_k^m d_k^m \frac{\frac{2\mathrm{i}}{\Delta t}}{\frac{\mathrm{i}}{\Delta t}+\frac{W_{\mathrm{l,r}}^{n+1}+d_k^m}{2}} \frac{\varphi_k^m(x_{\mathrm{l,r}})}{2} - \mathrm{sg}(\partial_{\mathbf{n}} W_{\mathrm{l,r}}^{n+1}) \frac{\sqrt{|\partial_{\mathbf{n}} W_{\mathrm{l,r}}^{n+1}|}}{2} \frac{\frac{2\mathrm{i}}{\Delta t}}{\frac{\mathrm{i}}{\Delta t}+\frac{W_{\mathrm{l,r}}^{n+1}}{2}} \frac{\psi^n(x_{\mathrm{l,r}})}{2}, \\
\varphi_k^{n+1}(x_{\mathrm{l,r}}) = \frac{\frac{\mathrm{i}}{\Delta t}-\frac{W_{\mathrm{l,r}}^{n+1}+d_k^m}{2}}{\frac{\mathrm{i}}{\Delta t}+\frac{W_{\mathrm{l,r}}^{n+1}+d_k^m}{2}} \varphi_k^n(x_{\mathrm{l,r}}) + \frac{1}{\frac{\mathrm{i}}{\Delta t}+\frac{W_{\mathrm{l,r}}^{n+1}+d_k^m}{2}} v^{n+1}(x_{\mathrm{l,r}}), \\
\psi^{n+1}(x_{\mathrm{l,r}}) = \frac{\frac{\mathrm{i}}{\Delta t}-\frac{W_{\mathrm{l,r}}^{n+1}}{2}}{\frac{\mathrm{i}}{\Delta t}+\frac{W_{\mathrm{l,r}}^{n+1}}{2}} \psi^n(x_{\mathrm{l,r}}) + \frac{\sqrt{|\partial_{\mathbf{n}} W_{\mathrm{l,r}}^{n+1}|}}{\frac{\mathrm{i}}{\Delta t}+\frac{W_{\mathrm{l,r}}^{n+1}}{2}} v^{n+1}(x_{\mathrm{l,r}}), \\
\varphi_k^0(x_{\mathrm{l,r}}) = \psi^0(x_{\mathrm{l,r}}) = 0,
\end{cases}
\tag{98}
$$

with $1 \leqslant k \leqslant m$, and $0 \leqslant n \leqslant N-1$.

We previously proved (see Proposition 7) that the schemes based on the discrete convolutions are unconditionally stable. It does not seem to be the case when rational Padé approximations are used. We do not have a proof of that result but let us explain why unconditional stability does not hold through numerical investigations. One of the key-points in Proposition 7 for proving the unconditional stability of the scheme based on convolution operators is that the application $F : z \mapsto F(z) := -\mathrm{i}\mathrm{e}^{-\mathrm{i}\pi/4}\sqrt{\frac{1-z}{1+z}}$ maps $\mathcal{C}(0,1)$ to $\mathbb{R}^- \cup i\mathbb{R}^-$. The analogous stability result for the Padé approximation would essentially be obtained by stating that it is also true for the application $F_m : z \mapsto F_m(z) := -i\mathrm{e}^{-\mathrm{i}\pi/4} R_m\left(\frac{1-z}{1+z}\right)$. Unfortunately, this does not seem to be true. In particular, the image is even not in the lower left quarter plane when z is close to the singular point -1. To illustrate this point, we draw in Fig. 4 the argument of both F and F_{50} and we also zoom near $z = -1$. As it can be seen, sign problems can arise prohibiting an *a priori* possible proof of an unconditional stability result.

4. Numerical examples

For the numerical simulations, we consider the initial gaussian datum: $u_0(x) = \mathrm{e}^{\mathrm{i}k_0 x - x^2}$, where k_0 designates the wave number fixed to: $k_0 = 10$ in our simulations. Concerning the spatial discretization, we use a variational formulation of the semi-discrete time problem for n_h elements (with size h) and integrate the ABCs in the scheme as a Fourier–Robin boundary condition.

We split our analysis in two parts: time independent and time dependent potentials.

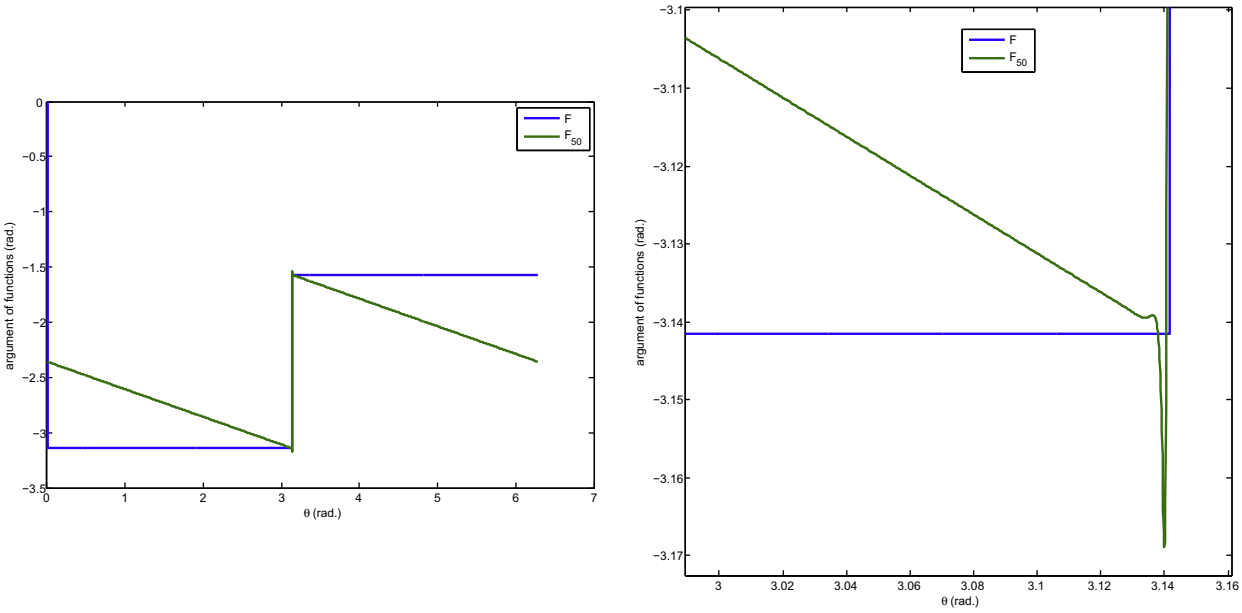

Fig. 4. Possible loss of stability for the rational Padé approximation. We compute the argument of $F(\mathrm{e}^{\mathrm{i}\theta})$ and $F_{50}(\mathrm{e}^{\mathrm{i}\theta})$ for $\theta \in [0; 2\pi]$ (left picture). We zoom near the point $z = -1$ in the right picture.

4.1. Time independent potentials

The first potential is given by a quadratic repulsive potential: $V_1(x) = x^2$. The computational domain is $\Omega =]-5; 15[$ and the final time of computation is $T = 2.5$.

We present in Fig. 5 the quantity $\log_{10}(|u(x,t)|)$ in the domain Ω_T. The linear finite element method uses 8×10^3 interior points (the space step is then $h = 2.5 \times 10^{-3}$) and the time step is $\Delta t = 10^{-4}$. We begin by representing the reference solution (top left) computed with an exact representation formula [9]. Next, we present (top) the solutions using ABC_0^2 and ABC_0^4 which show that increasing the order of the boundary conditions yields smaller spurious reflection. Next, we compare the effect of the localization based on the Padé approximation of order m for the second-order ABC. We choose $m = 20$ ($ABC_{1,20}^2$) and $m = 50$ ($ABC_{1,50}^2$) terms. To get an equivalent precision to ABC_0^2, $m = 50$ is required. However, we note here that this leads to a negligible additional cost compared to $m = 20$. We also see on the right bottom picture that the precision of ABC_0^4 is (at least) conserved for $ABC_{1,50}^4$.

To visualize and compare the parasitic reflection, we draw (in logarithmic scale) in Fig. 6 the values of the computed field $|u(x_l, t)|$ on the time interval $[0; T]$. The parameters are now $\Delta t = 10^{-4}$ and we take $n_h = 10^4$ finite elements. Again, according to the previous computations, we see the natural classification of the ABCs that we propose. We also observe that, for these discretization parameters, we obtain the lowest reflection equal to $10^{-5.5}$ for the fourth-order ABCs: ABC_0^4 and $ABC_{1,50}^4$. It is noticeable that a slightly lower reflection is visible for the Padé-based boundary conditions. It is in fact related to the discretization parameters. This is indeed confirmed in Fig. 7 where we present the logarithm of the maximum of the reflection at the left boundary for different time steps Δt according to the mesh refinement h. In particular, we can see that the Padé-type ABCs yield lower reflection for a given time step Δt compared to the convolution-based ABCs. This is an accuracy advantage of these ABCs which furthermore require less computational time. At the same time, we saw that no unconditional stability result is at hand for the Padé conditions. Finally, it is always much better to use a fourth-order condition than a second-order one.

Our second test considers the following potential: $V_2(x) = 5(2 + \cos x)$. We draw in Fig. 8 the amplitude (in logarithmic scale) of the computed fields in the computational domain $\Omega =]-10; 10[$, for $T = 2$. The discretization is fixed by $\Delta t = 10^{-4}$

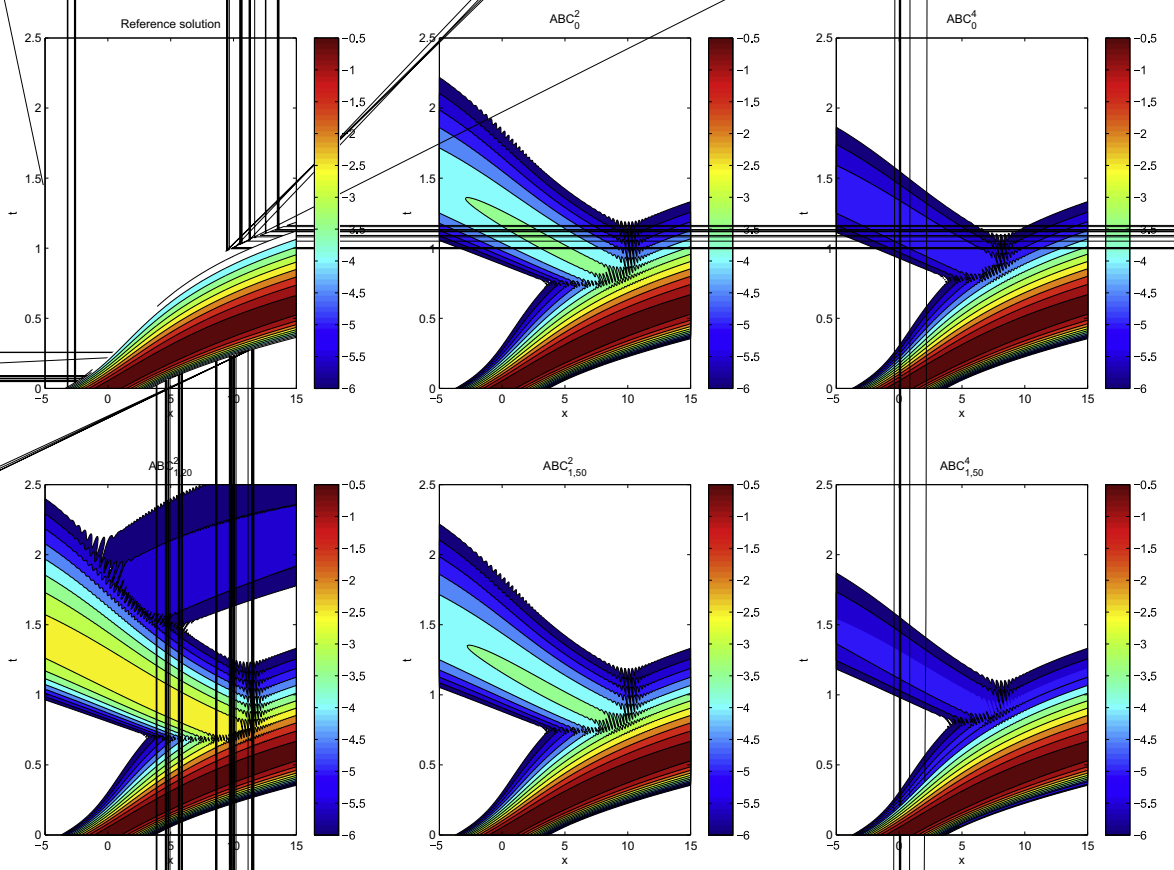

Fig. 5. $\log_{10}$ representation of the amplitude of the computed solutions for $V_1(x) = x^2$. From left to right, top: reference solution, ABC_0^2, ABC_0^4; bottom: $ABC_{1,20}^2$, $ABC_{1,50}^2$, $ABC_{1,50}^4$

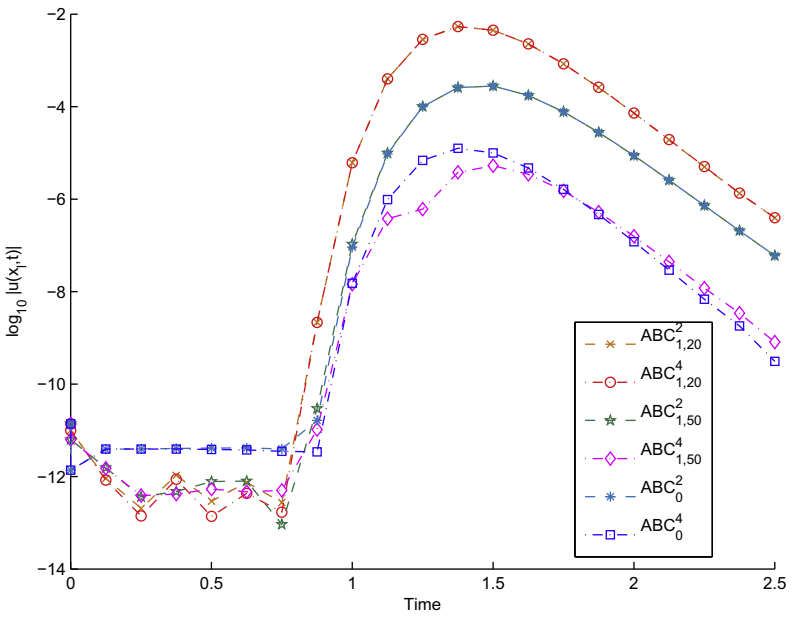

Fig. 6. Reflection at the left boundary for $V_1(x,t) = x^2$ and the different ABCs.

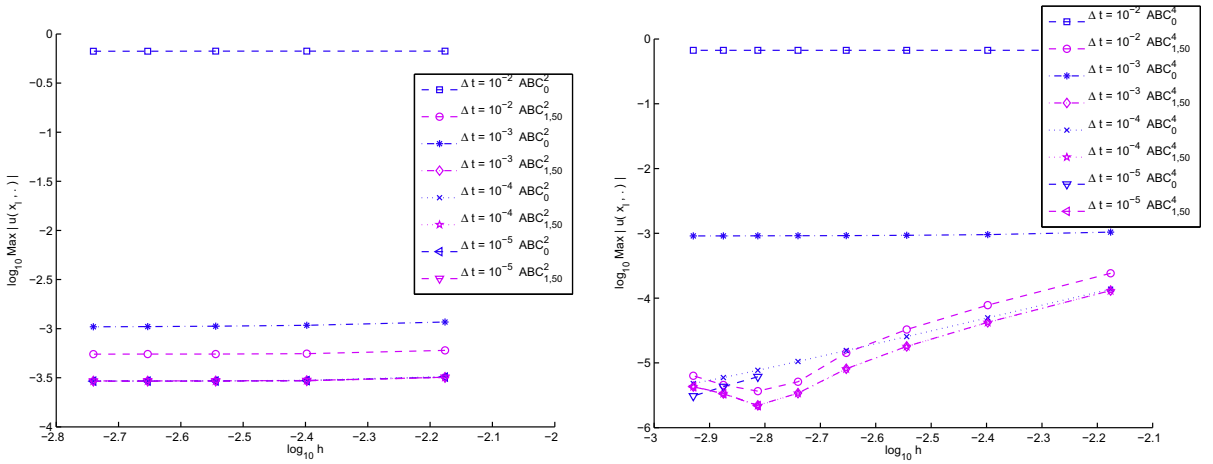

(a) Second-order ABCs (b) Fourth-order ABCs

Fig. 7. Maximum of the reflection at the left boundary for the different ABCs, according to the time step Δt and spatial mesh refinement h for $V_1(x) = x^2$.

and $n_h = 8 \times 10^3$. The reference solution for V_2 (and also for V_3 and V_4 in the next subsection) is computed on a larger domain to avoid any effect related to reflection at the boundary. The same comments apply as for V_1. Fig. 9 reports the maximum value of the reflection at the left boundary of the computational domain for the fourth-order ABCs, ABC_0^4 and $ABC_{1,50}^4$, with respect to Δt and h. We see that the reflection decreases with h and Δt and that it saturates around $10^{-4.8}$. Unlike for V_1, a given time discretization of an ABC leads to the same level of accuracy (for $\Delta t \leqslant 10^{-3}$).

4.2. Time dependent potentials

We consider now two time- and space-dependent potentials: $V_3(x,t) = 5xt$ and $V_4(x,t) = x(2 + \cos 2t)$.

In the first situation, we present in Fig. 10 the fields amplitude in the domain $[x_l, x_r] = [-5, 10]$ for a final time $T = 2.5$. The time step is $\Delta t = 5.10^{-4}$ and we use $n_h = 8 \times 10^3$. We see again the classification of the ABCs. Moreover,

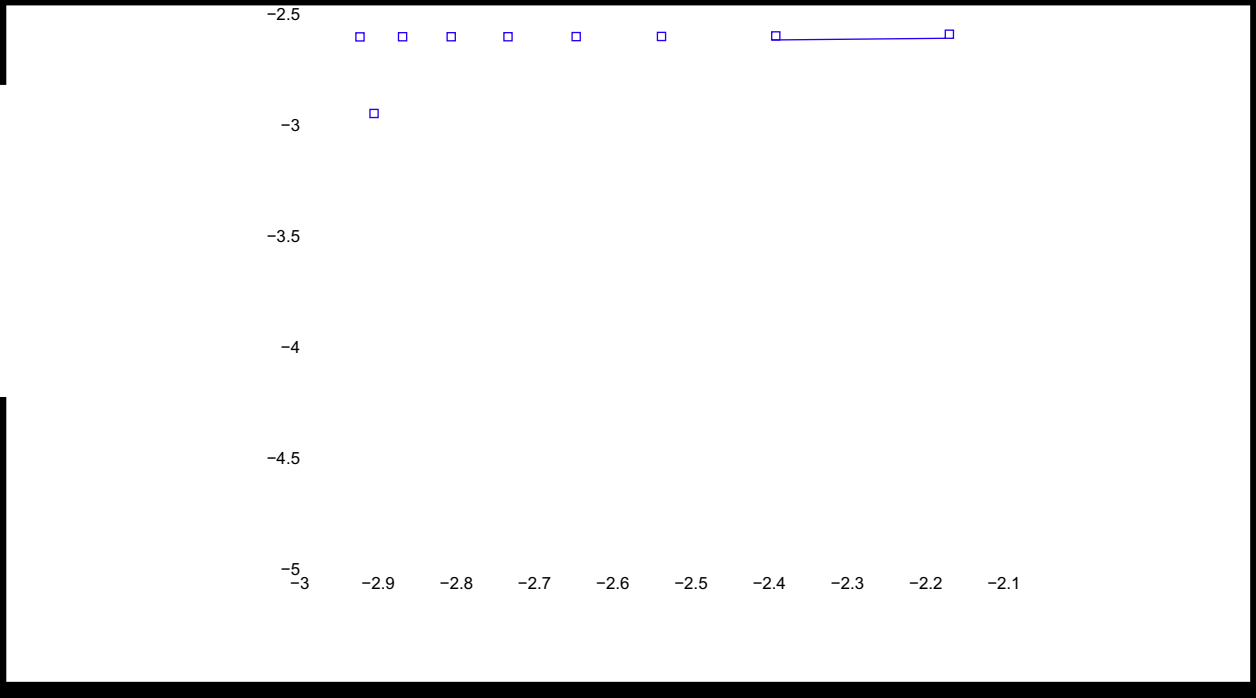
−2.5
−3
−3.5
−4
−4.5
−5
−3
−2.9
−2.8
−2.7
−2.6
−2.5
−2.4
−2.3
−2.2
−2.1

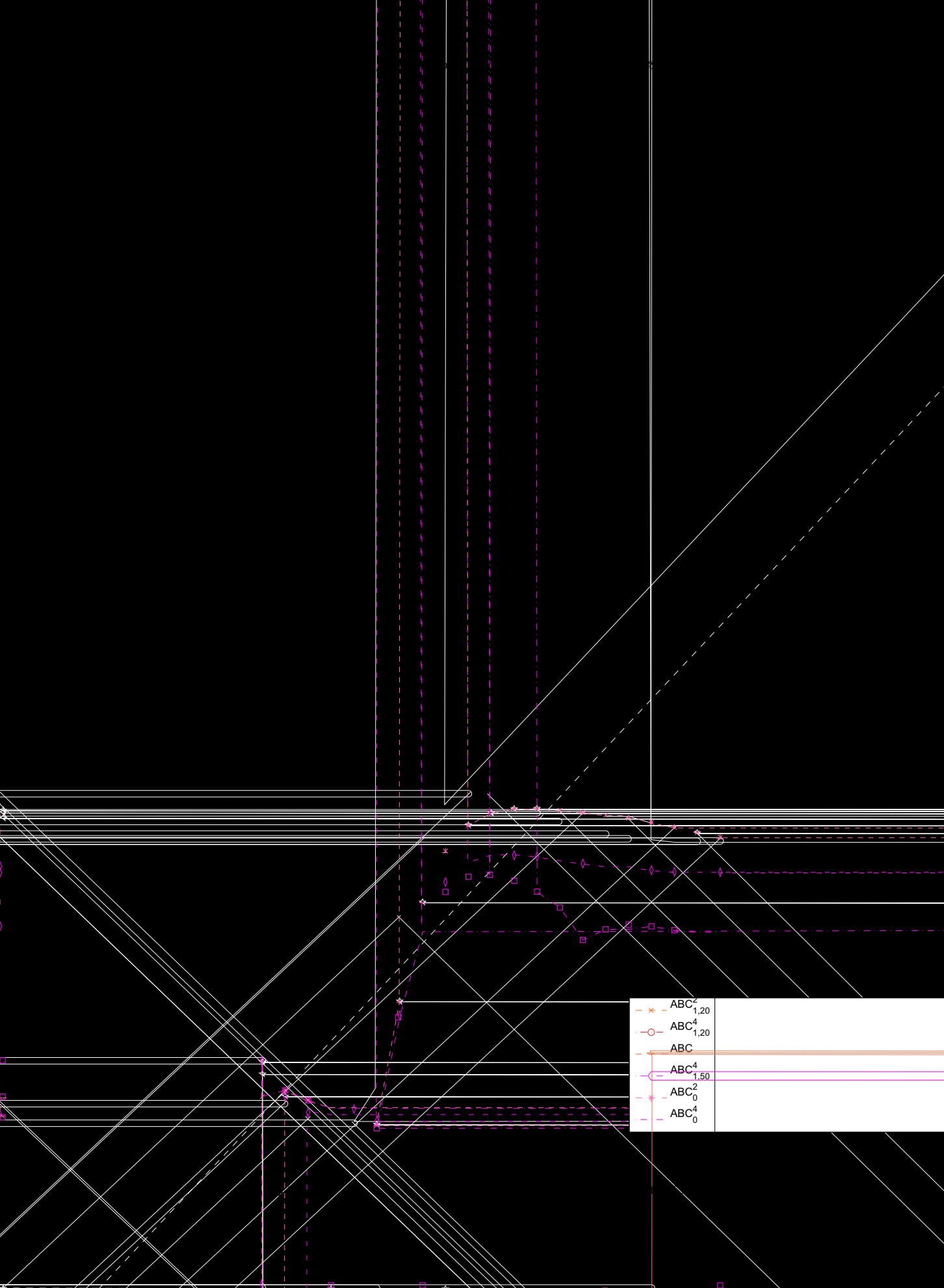
ABC 2 1,20
ABC 4 1,20
ABC
ABC 4 1,50
ABC 2 0
ABC 4 0

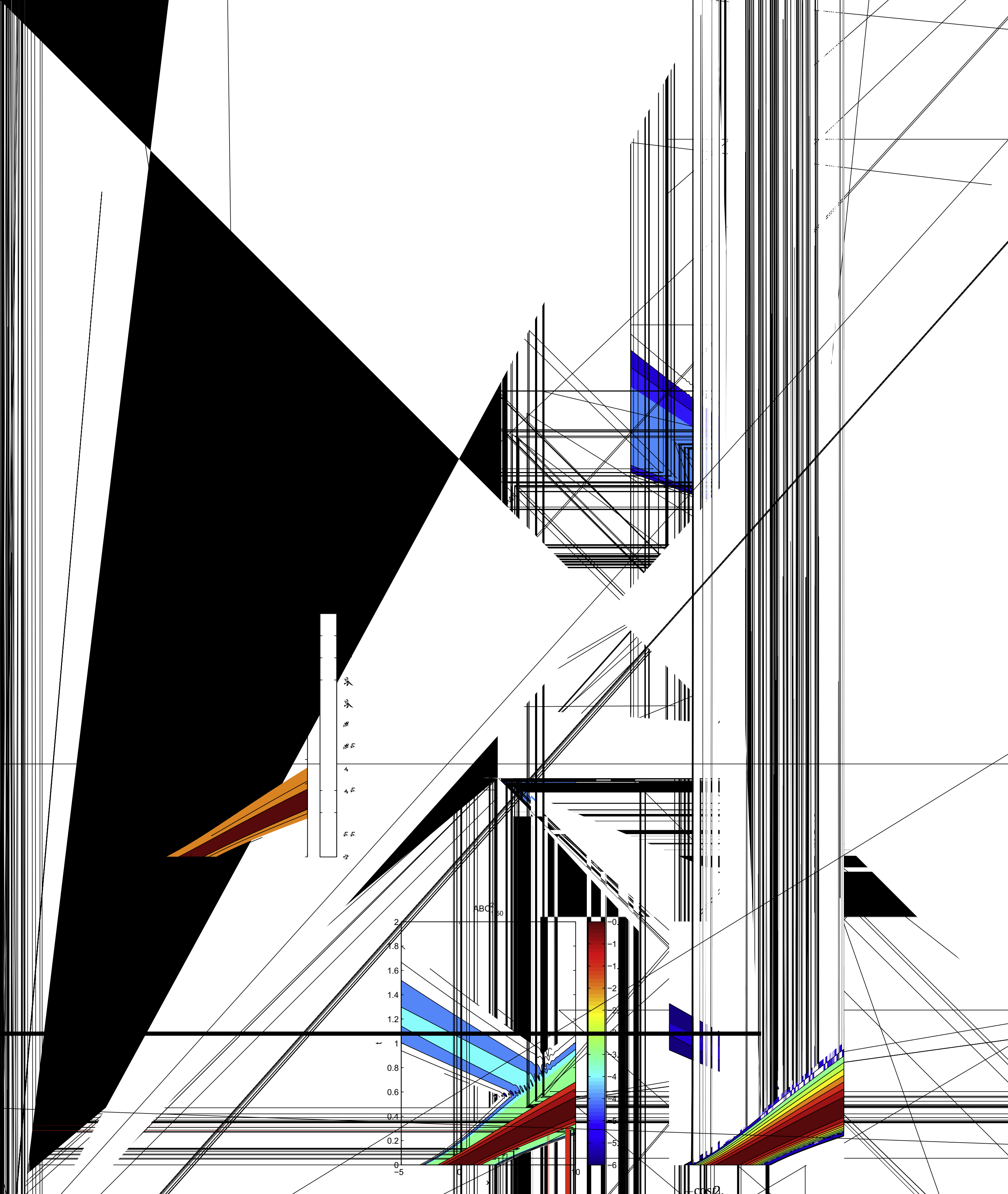

Fig. 13. Amplitude of the computed fields for the different ABCs for $V_4(x^t) = x^2 - \cos t 2$.

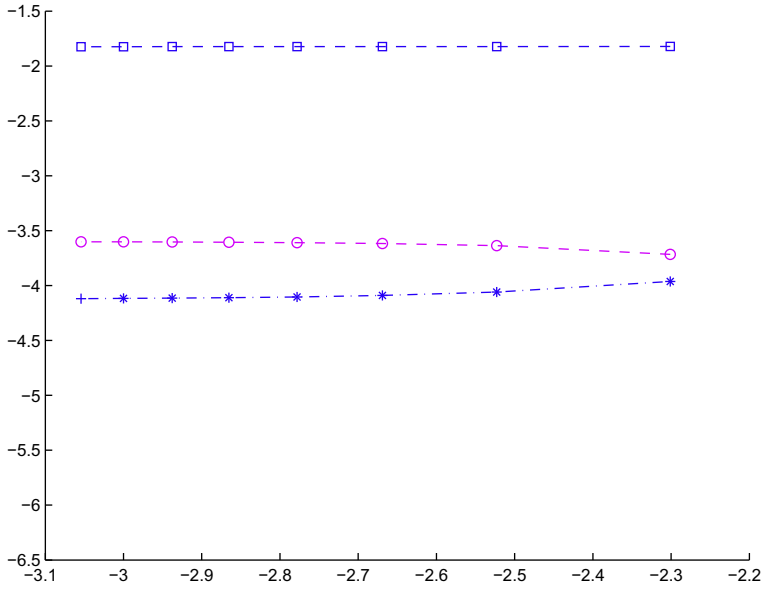

$[x_l, x_r] = [-5; 10]$). Fig. 12 draws the maximum of the reflection at the left endpoint for the fourth-order ABCs according to Δt and h.

We finally report in Figs. 13 and 14 the results obtained for V_4. For Fig. 13, we fix $\Delta t = 10^{-4}$ and $n_h = 10^4$. The domain of computation is: $[x_l, x_r] = [-5, 10]$ and the final time is $T = 2$. We see again that increasing the order of an ABC increases the accuracy. Unlike the previous case, $\mathrm{ABC}^4_{1,50}$ yields slightly lower reflection than ABC^4_0. This can also be observed in Fig. 14 for a given Δt.

5. Conclusion

This paper provides various constructions of Absorbing Boundary Conditions (ABCs) for the one-dimensional Schrödinger equation with time- and space-variable repulsive potentials. This kind of problems includes many interesting situations met in physics and applications. A complete mathematical analysis has been presented to emphasize the strengths and limitations of the different approaches. Next, a numerical analysis of associated unconditionally stable schemes has been fully developed. Numerical examples compare the different ABCs of various orders, showing that fourth-order ABCs yield accurate computations.

This work can be seen as a first step towards the derivation of more complex situations like higher-dimensional Schrödinger equations [6,16] (or also coupled systems of Schrödinger equations [29,28]) with potentials and nonlinearities. These present additional computational difficulties and will be the subject of forthcoming developments.

References

[1] M. Abramowitz, I.A. Stegun, Handbook of mathematical functions with formulas, graphs, and mathematical tables, 10th Printing, Volume 55 of National Bureau of Standards Applied Mathematics Series, For Sale by the Superintendent of Documents, US Government Printing Office, Washington, DC, 1964.
[2] X. Antoine, A. Arnold, C. Besse, M. Ehrhardt, A. Schädle, A review of transparent and artificial boundary conditions techniques for linear and nonlinear Schrödinger equations, Commun. Comput. Phys. 4 (4) (2008) 729–796.
[3] X. Antoine, C. Besse, Construction structure and asymptotic approximations of a microdifferential transparent boundary condition for the linear Schrödinger equation, J. Math. Pures Appl. (9) 80 (7) (2001) 701–738.
[4] X. Antoine, C. Besse, Unconditionally stable discretization schemes of non-reflecting boundary conditions for the one-dimensional Schrödinger equation, J. Comput. Phys. 188 (1) (2003) 157–175.
[5] X. Antoine, C. Besse, S. Descombes, Artificial boundary conditions for one-dimensional cubic nonlinear Schrödinger equations, SIAM J. Numer. Anal. 43 (6) (2006) 2272–2293 (Electronic).
[6] X. Antoine, C. Besse, V. Mouysset, Numerical schemes for the simulation of the two-dimensional Schrödinger equation using non-reflecting boundary conditions, Math. Comput. 73 (248) (2004) 1779–1799 (Electronic).
[7] A. Arnold, Numerically absorbing boundary conditions for quantum evolution equations, VLSI Design 6 (1–4) (1998) 313–319.

[8] J. Bony, R. Carles, D. Häfner, L. Michel, Scattering theory for the Schrödinger equation with repulsive potential, J. Math. Pures Appl. 84 (5) (2005) 509–579.
[9] R. Carles, Linear vs. nonlinear effects for nonlinear Schrödinger equations with potential, Commun. Contemp. Math. 7 (4) (2005) 483–508.
[10] R. Carles, Semi-classical analysis for nonlinear Schrödinger equations, World Scientific, 2008.
[11] G. Doetsch, Anleitung zum praktischen Gebrauch der Laplace-Transformation und der $\mathcal{Z}$-Transformation, vol. 3. Auflage. R. Oldenburg Verlag Munchen, Wien, 1967.
[12] M. Ehrhardt, R. Mickens, Solutions to the discrete Airy equation: Application to parabolic equation calculations, J. Comput. Appl. Math. 172 (2004) 183–206.
[13] M. Ehrhardt, C. Zheng, Exact artificial boundary conditions for problems with periodic structures, J. Comput. Phys. 227 (2008) 6877–6898.
[14] M. Ehrhardt, A. Zisowsky, Fast calculation of energy and mass preserving solutions of Schrödinger–Poisson systems on unbounded domains, J. Comput. Appl. Math. 187 (2006) 1–28.
[15] B. Engquist, A. Majda, Absorbing boundary conditions for numerical simulation of waves, Math. Comp. 31 (1977) 629–651.
[16] H. Han, D. Yin, Z. Huang, Numerical solutions of Schrödinger equations in $\mathbb{R}^3$, Numer. Meth. Partial Diff. Equat. 23 (2006) 511–533.
[17] R. Lascar, Propagation des singularités des solutions d'équations pseudo-différentielles quasi-homogènes, Ann. Inst. Fourier (Grenoble) 27 (2) (1977) 79–123.
[18] M. Levy, Parabolic equation methods for electromagnetic wave propagation, Volume 45 of IEE Electromagnetic Waves Series, Institution of Electrical Engineers (IEE), London, 2000.
[19] E. Lindmann, Free-space boundary conditions for the time dependent wave equation, J. Comput. Phys. 18 (1985) 16–78.
[20] E. Lorin, A. Bandrauk, S. Chelkowski, Numerical Maxwell–Schrödinger model for laser-molecule interaction and propagation, Comput. Phys. Commun. 177 (12) (2007) 908–932.
[21] E. Lorin, S. Chelkowski, A.D. Bandrauk, Mathematical modeling of boundary conditions for laser-molecule time dependent Schrödinger equations and some aspects of their numerical computation – one-dimensional case, Numer. Meth. for P.D.E., in press.
[22] F. Milinazzo, C. Zala, G. Brooke, Rational square-root approximations for parabolic equation algorithms, J. Acoust. Soc. Am. 101 (2) (1997) 760–766.
[23] J. Muga, J. Palao, B. Navarro, I. Egusquiza, Complex absorbing potentials, Phys. Rep. – Rev. Sect. Phys. Lett. 395 (6) (2004) 357–426.
[24] L. Nirenberg, Pseudodifferential operators and some applications, Volume 17 of Regional Conference Series in Mathematics AMS 17, Lectures on Linear Partial Differential Equations, AMS, 1973.
[25] C. Zheng, Approximation, stability and fast evaluation of exact artificial boundary condition for the one-dimensional heat equation, J. Comput. Math. 25 (6) (2007) 730–745.
[26] C. Zheng, A perfectly matched layer approach to the nonlinear Schrödinger wave equations, J. Comput. Phys. 227 (2007) 537–556.
[27] C. Zheng, An exact absorbing boundary condition for the Schrödinger equation with sinusoidal potentials at infinity, Commun. Comput. Phys. 3 (3) (2008) 641–658.
[28] A. Zisowsky, Discrete transparent boundary conditions for systems of evolution equations, Ph.D. Thesis, TU Berlin, 2003.
[29] A. Zisowsky, A. Arnold, M. Ehrhardt, T. Koprucki, Discrete transparent boundary conditions for transient kp-Schrödinger equations with application to quantum-heterostructures, J. Appl. Math. Mech. (ZAMM) 85 (2005) 793–805.